Supplementary Materials for

Small Molecule–Mediated Precision Protein Editing in living cells

Ge Sun,[1,2,7] Jin Lin,[3,7] Zhicheng Yang,[2,7] Jie Yang,[4,7] Yiran Hu,[2,5,7] Fei Ye,[6,7] Yizhou Bian,[3] Shuiping Fu,[2] Yifan Ma,[2] Zhenyu Wang,[2] Ziteng Li,[2] Junyi Qiu,[1] Hu Zhou,[2,*] Hua Lin,[4,*] Cheng Luo[1-3,5,*]

[1]State Key Laboratory of Discovery and Utilization of Functional Components in Traditional Chinese Medicine, Guizhou Provincial Key Laboratory of Digestive System Diseases, The Affiliated Hospital of Guizhou Medical University, Guiyang, 561113, China
[2]State Key Laboratory of Drug Research, Shanghai Institute of Materia Medica, Chinese Academy of Sciences, 555 Zuchongzhi Road, Shanghai, 201203, China
[3]The School of Pharmacy, Fujian Medical University, Fuzhou, 350122, China
[4]key Laboratory of Microbial Pathogenesis and Interventions of Fujian Province University, the Key Laboratory of Innate Immune Biology of Fujian Province, Biomedical Research Center of South China, College of Life Sciences, Fujian Normal University, Fuzhou, 350117, China
[5]Hangzhou Institute for Advanced Study, University of Chinese Academy of Sciences, Hangzhou, 310024, China
[6]College of Life Sciences and Medicine, Zhejiang Sci-Tech University, Hangzhou, 310018, China
[7]These authors contributed equally：Ge Sun, Jin Lin, Zhicheng Yang, Jie Yang, Yiran Hu, Fei Ye
[*]Correspondence author. Email: zhouhu@simm.ac.cn; hlin@fjnu.edu.cn; cluo@simm.ac.cn

Methods:

Spectral measurements

Photoluminescence spectra were recorded on a spectrofluorometer (Agilent Cary Eclipse) with a quartz absorption cuvette (light path: 1 cm). Samples were prepared with 0.1 mM photocatalysts in DMF. Each emission spectrum was recorded at an excitation wavelength of 350 nm and was corrected according to the calibration factors of the instrument. Results are shown in Supplementary Fig. S7c.

Cyclic voltammetry experiments

Cyclic voltammetry (CV) measurements were performed using a CHI (model 600E) electrochemical analyzer/workstation. A three-electrode setup was used, consisting of a glassy carbon working electrode, platinum wire counter electrode, and Ag/AgCl reference electrode. Samples were prepared with 1 mM photocatalysts and 100 mM $TBAPF_6$ electrolyte solution in DMF, and deaerated by sparging with nitrogen for at least 5 minutes before performing measurements with a scan rate of 100 mV/s. All data are recorded with reference to Ag/AgCl. Results are shown in Supplementary Fig. S7d.

Protein expression and purification

GST-CDK2 and its mutant D145A were expressed in E. coli BL21 (DE3) cells in 2×YT (2× yeast extract-tryptone) medium. The bacterial culture was incubated at 37 ℃ until the OD600 reached 0.8. Then, the temperature was reduced to 16 ℃, and induction with 0.4 mM IPTG proceeded for 16 h before harvesting by centrifugation. Cell pellets were resuspended in lysis buffer (50 mM HEPES pH 7.4, 200 mM NaCl, and 5 mM β-mercaptoethanol (BME)) and subjected to ultrasonication for disruption. GST-CDK2 was purified by GSTrapTMHP column (GE Healthcare). The GST tag was cleaved overnight at 4°C with PPase. Following cleavage, the sample was reloaded onto GST Trap column to remove the GST tag, and the flow-through containing the cleaved protein was further purified by Superdex75 10/300 GL column (GE Healthcare) into the crystal buffer (20 mM HEPES pH 7.4, 100 mM NaCl, 2 mM DTT).

The FGFR2 kinase domain was expressed in E. coli BL21 (DE3) cells grown in liquid LB medium. The bacterial culture was incubated at 37 ℃ until the OD600 reached 0.8, after which

the temperature was lowered to 16 °C. Protein expression was induced with 1 mM IPTG for 16 h before harvesting the cells by centrifugation. The resulting cell pellets were resuspended in lysis buffer and subjected to ultrasonication for cell disruption. Proteins were purified using nickel affinity chromatography (HisTrap HP, 5 mL, GE Healthcare) on an ÄKTA Pure system. The purity of the proteins was assessed by SDS-PAGE, followed by concentration to the desired levels and storage in Buffer B (20 mM HEPES, pH 7.5, 200 mM NaCl, and 5% glycerol) at −80 °C for subsequent assays.

The GST-CDK12(714-1063)/GST-CCNK(1-267) complex was subcloned into pFBDM vector and expressed in SF9 insect cells using the baculovirus expression system. The cells were collected then resolved in 50 mM Tris–HCl (pH 8.0), 400 mM NaCl, 10% (v/v) glycerol, 1mM DTT, 1 mM phenylmethylsulfonylfluoride (PMSF), and 1× protease inhibitor cocktail (MCE). Following lysis and ultracentrifugation, the soluble fraction was passed over GSTrapTMHP column, washed with 50 mM Tris–HCl pH 8.0, 400 mM NaCl, 10% glycerol, 1 mM TCEP and 20 mM Glutathione. The affinity tags were removed with GST-Tobacco Etch Virus (TEV) protease overnight at 4°C. After removal of GST-TEV and GST-tag, the complex was further purified by Superdex75 10/300 GL column with Hepes7.5 20mM, 400mM NaCl.

Molecular-level editing operations

Proteins were desalted into PBS buffer using desalting column. To a PBS buffer solution (89 μL) was added 10 μL of protein solution (500 μM) and 1 μL of compound (5 mM), giving a final compound/protein ratio of 1:1. The sample were mixed and incubated at room temperature (25 ºC) for 5 min. The sample was transferred into a custom quartz glass tube, and the air inside the tube was replaced with inert gas. The quartz glass tube was then irradiated at 400-405 nm for 12 h (4 ºC).

Protein Thermal Shift (PTS)

PTS assays were conducted on the QuantStudio™ 6 Flex real-time PCR instrument (Applied Biosystems). Final concentration of 5 μM CDK2 protein, 4× SYPRO orange dye (Invitrogen) and compounds were mixed in PTS buffer (20 mM HEPES pH 7.4, 150 mM NaCl) under light-protected conditions. Each well of the reaction system contained 20 μL and the mixture was centrifuged at 1500 rpm for 2 minutes. The temperature was then linearly increased from 25 °C to

95 °C over 24 minutes. Data were analyzed using the Protein Thermal Shift TM software (Applied Biosystems, Version 1.2) to determine the Tm value. The temperature-fluorescence intensity curve, also known as the protein melting curve was plotted with GraphPad Prism 8.2. Results are shown in Supplementary Fig.S9.

Enzymatic activity assay for CDK

The enzymatic activity assay for CDKs was conducted utilizing the Lance Ultra Assay. The test compounds were diluted in kinase assay buffer (50 mM HEPES, pH 7.5, 0.0015% Brij-35) and thoroughly mixed for 10 min to ensure homogeneity. In a 384-well assay plate, 5 μL of the diluted compound solution was combined with 10 μL of the CDKs solution and incubated at room temperature for 10 min. The kinase reaction was initiated by adding 10 μL of the 2.5X FAM-labeled peptides and ATP mixture at 28 °C for specified time. The reaction is then quenched by 25 μL stopping solution (100 mM HEPES, pH 7.5, 0.015% Brij-35, 0.2% Coating Reagent #3, 50 mM EDTA). The data is acquired using Caliper (PerkinElmer, Caliper EZ ReaderII), followed by subsequent analysis and curve fitting to determine the inhibitory IC_{50} value of the compound. Results are shown in Supplementary Fig. S10.

Crystallization and X-ray data collection

CDK2 protein were crystallized by mixing equal volume of protein (10 mg / mL) and the reservoir solution (HEPEs pH 7.5, 15% PEG3350) using the hanging drop vapor diffusion method at 16 °C. The cocrystal of CDK2 with **LL-DA-3** or **LL-DA-4** were obtained via soaking the compound into apo CDK2 crystal. To cryoprotect the crystals in liquid nitrogen, 25% ethylene glycol was added into the reservoir solution. Diffraction data were collected at 100 K on beamlines BL19U1 at the Shanghai Synchrotron Radiation Facility.[1]

Structure determination and refinement

Mtz files were obtained by utilizing the built-in XIA2_XDS program at the Shanghai Synchrotron Radiation Facility. Molecular replacement was performed using the Phaser-NR (full-featured) module of Phenix and coordinates from PDB entry 2VU3. The structure of **LL-DA-3** or **LL-DA-4** was drawn in ChemDraw. The cif and pdb files of compound were generated by Elbow

module of Phenix. Final structures were obtained through Phenix's Refine program. The validation of the final model was performed by PyMol. Results are shown in Supplementary Figs. S12-13.

Biolayer Interferometry (BLI) binding assay

To assess the binding affinity between the CDK2 and compounds, the BLI assay was performed on a OCTET R8 (SARTORIUS) using super streptavidin (SSA) biosensors at 25 °C. The CDK2 protein was first biotinylated and subsequently immobilized onto SSA sensors. The immobilization procedure was performed by sequentially running the following steps: Baseline (60 s), Loading (600 s), and Baseline (60 s). In parallel, an equivalent number of SSA sensors were used as reference channels, which were not subjected to protein immobilization. Subsequently, six different concentrations (50 μM, 16.7 μM, 5.56 μM, 1.85 μM, 0.62 μM, 0.21 μM) of compound were prepared and added to 96-well plate. The running buffer contained 1×PBS, 0.02% Tween-20 and 1% DMSO. The protein-small molecule association and dissociation kinetics were measured using a four-step sequential procedure: Equilibrium (450 s), Baseline (60 s), Association (300 s), and Dissociation (400 s). BLI data were analyzed by Octet® Analysis Studio. The equilibrium dissociation constant KD was calculated by steady state analysis using a 1:1 Langmuir binding model. Results are shown in Supplementary Fig. S8.

Cell-level editing operations

The human embryonic kidney 293T was purchased from American Type Culture Collection (Manassas, USA). 293T was maintained according to the provider' instructions. When the cells reached 70% confluence, they were transfected with PEI reagent to overexpress Flag-CDK2 protein. After transfection for 36 h, the culture medium was replaced with fresh medium containing 10 μM LL-DA-3, and the cells were incubated for 2 h at 37 °C. Subsequently, without removing the drug-containing medium, the cells were irradiated under 400-405 nm light for 2 h. After irradiation, the medium was removed and the cells were washed three times with ice-cold PBS. Then, the cells were lysed, and the supernatant was collected. Flag beads were added to the supernatant, and the mixture was incubated overnight to enrich CDK2 protein for subsequent mass spectrometry analysis.

Kinase Panel assay

The kinase selectivity of compound on the kinase panel was evaluated using Homogeneous Time-Resolved Fluorescence (HTRF) or ADP-Glo assay conducted by ICE Bioscience Inc, Beijing. 100× of the compound to be tested was transferred to a 384-well plate using Echo® Liquid Handler (ECHO), followed by the addition of 2× kinase and metal solution, centrifugation at 1000 rpm for 1 minute, and incubation at 25°C for 10 minutes. 2× substrate and ATP solution prepared in kinase buffer was added to 384-well plate, centrifugation at 1000 rpm for 1 minute, and incubation at 25°C for 60 minutes. In the HTRF assay, the kinase detection reagent contained XL665 and antibody. The fluorescence signals of 620 nm (Cryptate) and 665 nm (XL665) were read by PHERAstar microplate reader, calculate the ratio of 665 to 620. In the ADP-Glo assay, the luminescence signals of ADP-Glo reagent were recorded on PHERAstar microplate reader.

The vehicle control is 1% DMSO, and the positive control is 10 μM of the positive Control Article. The inhibition rate for each reaction well is calculated according to the formula:

$$\% \text{ Inhibition} = \left[1 - \frac{\overline{\text{Data}}_{\text{Cmpd}} - \overline{\text{Data}}_{\text{positive}}}{\overline{\text{Data}}_{\text{vehicle}} - \overline{\text{Data}}_{\text{positive}}}\right] \times 100$$

$\overline{\text{Data}}_{\text{positive}}$: The average Ratio for the positive controls (10 μM Positive Control Article)

$\overline{\text{Data}}_{\text{vehicle}}$: The average Ratio for the vehicle controls (1% DMSO)

The selectivity of the compounds was assessed by establishing a screening model for the evaluation of the selectivity of 80 kinase targets, and the inhibition of the compounds on the targets was evaluated by ADP-Glo and HTRF methods. Kinases are marked with dots, where the color of each kinase indicates the level of inhibition achieved by the compound, with color coding as follows: red signifies 90-100% inhibition, yellow indicates 80-90%, blue represents 70-80%, and light blue denotes 50-70%. Green implies inhibition below 50% and no significant inhibition of the target. This detailed visualization aids in identifying the selectivity profile of the compound, highlighting its potential therapeutic targets and off-target effects, which are critical for drug development and safety assessments. Results are shown in Supplementary Figs. S3-4 and S18.

LC-MS/MS Analysis for the Identification and Semi-Quantitation of Editing Sites

The reaction mixture was first subjected to high-speed centrifugation at 15,000 × g for 20 minutes at 4 °C. Subsequently, a filtration-assisted enzymatic digestion (FASP[2])procedure was employed to digest intact proteins into peptides. Specifically, 10 μL of the reaction solution (approximately 15 μg) was transferred into a centrifugal filter unit with a molecular weight cutoff

of less than 10 kDa. Prior to use, the filter units were pre-loaded with 200 μL of 100 mM TEAB (pH 8.5). The loaded samples were centrifuged at 12,000×g for 30 minutes at 4 °C, after which an additional 200 μL of 100 mM TEAB (pH 8.5) was added and the centrifugation step was repeated at 12,000 × g for 30 minutes at 4 °C. This washing procedure was repeated twice. Finally, 200 μL of 100 mM TEAB (pH 8.5) was added, and 1 μg of sequencing-grade trypsin was spiked into the sample. The enzymatic digestion was carried out at 37 °C for 16 hours.

Upon completion of the digestion, 20 μL of 10% TFA was added to acidify the sample, followed by centrifugation at 12,000 × g for 10 minutes. Desalting was performed using in-house prepared C18 desalting tips. The procedure for desalting was as follows: A small disk was punched out from a C18 disk using a blunt-end syringe needle and transferred into a 200 μL pipette tip. The tip was pre-conditioned sequentially with 200 μL methanol, 200 μL of 60% ACN/0.1% TFA, and twice with 200 μL of 0.2% TFA. The sample was loaded onto the tip, washed twice with 0.2% TFA, and the peptides were subsequently eluted with 90% ACN/0.2% TFA. The eluate was lyophilized and stored at –80 °C until analysis. Prior to LC-MS/MS analysis, the peptides were reconstituted in 10 μL of 0.1% FA and quantified at A205 using a Nanodrop instrument, with 1 μg of peptides being injected for analysis.

The LC-MS/MS analysis was performed using an EASY-nLC1200 system (self-packed column: 75 μm × 150 mm; 3 μm ReproSil-Pur 120 C18-AQ) coupled with a Q Exactive HF mass spectrometer. The liquid chromatography conditions were as follows: peptides were separated by a 60-minute gradient at a flow rate of 300 nL/min. Mobile phase A consisted of 0.1% (v/v) formic acid in water, and mobile phase B consisted of 0.1% (v/v) formic acid in 80% acetonitrile. The gradient was set as follows: 1 minute at 2%–4% B; 46 minutes at 4%–26% B; 6 minutes at 24%–35% B; 3 minutes at 35%–90% B; with 90% B maintained for 6 minutes. Mass spectrometry parameters were configured as follows: For MS1 scans, peptides were analyzed at a resolution of 60,000, with an AGC target of 1,000,000, a maximum injection time of 450 ms, and a scan range of 100–1500 m/z. The top 10 precursor ions were selected for fragmentation using an isolation window of 1.7 m/z and subjected to HCD at 27% NCE. MS2 scans were recorded at a resolution of 60,000 with an AGC target of 100,000 and a maximum injection time of 220 ms. A dynamic exclusion of 30 seconds was applied. The raw MS data were processed with MaxQuant, Skyline, BiopharmFinder, and pFind to determine protein editing sites, which were visualized using GP-Plotter[3]. For quantification, extracted ion chromatogram (XIC) peak areas at the MS1 level

corresponding to the edited and unedited peptide species were obtained using Skyline. Editing ratios were calculated by comparing the MS1 peak area of the edited peptide to the summed peak areas of the edited and unedited peptides with identical backbone sequences, enabling semi-quantitative estimation of editing efficiency. Results are shown in Supplementary Figs. S5-7, 15-17.

LC-MS/MS Analysis for the Identification of Intracellular Editing Sites

Following washing, the magnetic beads were re-suspended in 200 μL of 100 mM TEAB (pH 8.5) digestion buffer, and 1 μg of sequencing-grade trypsin was added. The digestion was carried out at 37 °C for 16 hours. After the digestion, the peptide-containing supernatant was transferred to a new tube, 20 μL of 10% TFA was added to acidify the sample, and the mixture was centrifuged at 12,000 × g for 10 minutes. Desalting was performed using in-house prepared C18 tips, followed by lyophilization of the peptides and storage at –80 °C until LC-MS/MS analysis. Prior to analysis, peptides were reconstituted in 25 μL of 0.1% FA and quantified at A205 using a Nanodrop instrument; 200 ng of peptides was injected for LC-MS/MS analysis.

The LC-MS/MS analysis was carried out using a Vanquish Neo system coupled to an Orbitrap Astral mass spectrometer. The liquid chromatography was operated in trap-and-elute mode with a trap column (PepMap Neo) and an analytical column (self-packed column: 100 μm × 100 mm; 1.9 μm ReproSil-Pur 120 C18-AQ). Peptides were eluted over a 25-minute gradient at a flow rate of 2.2 μL/min. Mobile phase A was comprised of 0.1% (v/v) formic acid in water, and mobile phase B consisted of 0.1% (v/v) formic acid in 80% acetonitrile. The gradient conditions were as follows: 16.2 minutes at 0%–30% B; 3 minutes at 30%–40% B; 2.5 minutes at 40%–99% B; and a 3.3-minute hold at 99% B.

For mass spectrometry, MS1 scans were performed at a resolution of 240,000 with an AGC target of 5,000,000, a maximum injection time of 5 ms, and a scan range of 150–1700 m/z, with a cycle time of 1.2 s. An isolation window of 1.6 m/z was used for fragmentation via HCD at 27% NCE. MS2 scans were acquired with an AGC target of 500,000 and a maximum injection time of 10 ms. A dynamic exclusion of 12 seconds was applied. Raw MS data were processed with MaxQuant to determine intracellular protein editing sites, which were visualized using GP-Plotter. Furthermore, the peak areas of the peptides were extracted using Skyline for a preliminary quantification to estimate the editing ratios. Results are shown in Fig 1g.

Quantum chemistry calculations

The mechanism of chemical editing has been investigated using the quantum chemical cluster method that has been successfully applied to enzyme reaction mechanism calculations [4, 5]. The condensation reaction model was constructed based on the **LL-DA-3**-CDK2 complex structure. For the cluster model of the CDK2, the residues within 5 Å of the active site were reserved, which contains **LL-DA-3**, key residues D145, K33, N132, other skeleton residues as well as six water molecules near the catalytic center, leading to 265 atoms in total. Subsequently, density functional theory (DFT) with the B3LYP-D3 functional was subjected to quantum chemistry calculations, using the Gaussian16 software package [6-8]. The 6-311G** basis set was used for the geometry optimizations, followed by frequency calculations of the optimized geometries to obtain zero-point energy (ZPE) corrections. The geometry optimizations for transition states (TSs) and intrinsic reaction coordinate (IRC) were also performed at B3LYP-D3/6-311G** level. Afterwards, single point energy calculations for each minimum were carried out using 6-311+G** basis set. Then we used the shermo program to calculate the thermodynamic data for the system [9]. In order to obtain more accurate free energy results, we have also calculated the free energy of dissolution of the system. The calculation of the dissolution free energy was performed based on the Solvation Model Based on Density (SMD) at the B3LYP-D3/6-311+G** level [10]. Results are shown in Supplementary Fig. S14.

Statistical analysis

GraphPad Prism 8 (GraphPad Software, v.8.0.1) was used for visualizations and to calculate ignificant differences. Sample sizes (n) refer to biological replicates. For in vitro studies, replicates indicate independent biological samples randomly allocated into experimental groups.

Chemistry Experiment

Starting materials, reagents, and solvents were purchased from commercial suppliers and were used without further purification unless otherwise stated. Reactions were monitored by thin-layer chromatography (precoated silica gel F254 plates, HSGF254) and UPLC/MS system (UltiMate 3000 + LCQ Fleet). Compounds were purified by Flash column chromatography with Teledyne ISCO CombiFlash Rf system using prepacked columns. All final compounds were purified by

Semi-preparative HPLC system using XBridge® Prep C18 column (19 x 250 mm, 5 μm particle size). The analytical method was as follows: flow rate, 10 mL/min; solvent A = MeCN; solvent B = 0.1% TFA in water; solvent gradient = 5% A to 95% A in 30 min, 95 % A in 30-45 min; UV detection at 254 nm.). ^{1}H NMR spectra were recorded on 400 and 500 and 800 MHz Bruker Avance spectrometer, or 600 MHz JEOL ECZ spectrometer. ^{13}C NMR spectra were recorded on 101 and 125 and 200 MHz Bruker Avance spectrometer, or 151 MHz JEOL ECZ spectrometer. Chemical shifts were reported in parts per million (ppm, δ) downfield from tetramethylsilane (TMS). Coupling constants (J) were reported in Hz. Spin multiplicities were described as brs (broad), s (singlet), d (doublet), t (triplet), q (quartet) and m (multiplet). High-resolution mass spectra (HRMS) data were acquired in the positive ion mode using UPLC/MS system (UltiMate 3000 + Q Exactive Rocus) with an electrospray ionization (ESI) source. The purity of all final compounds was confirmed to be greater than 95% by NMR and UPLC/MS system. The analytical method was as follows: flow rate, 0.8 mL/min; eluent A, neutral acetonitrile; eluent B, 0.1% formic acid in water; gradient, 5% A to 95% A in 5 min; UV detection at 254 nm.

Scheme 1. Synthesis of LL-DA-1~4

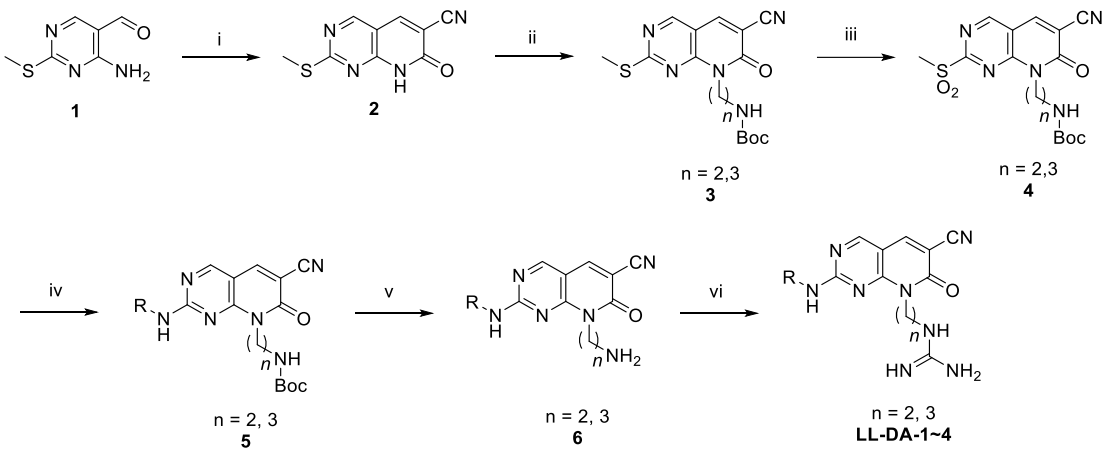

Reagents and conditions: (i) $CNCH_2CO_2H$, $BnNH_2$, AcOH, 100°C; (ii) bromide, NaH, DMF, r.t.; (iii) *m*-CPBA, CH_2Cl_2, 0°C-r.t.; (iv) amine, DMF, TEA, r.t.; (v) TFA, CH_2Cl_2, 0°C-r.t.; (vi) 1H-pyrazole-1-carboxamidine hydrochloride, DMF, TEA, r.t..

Procedure for the preparation of 2-methylsulfanyl-7-oxo-7,8-dihydropyrido[2,3-*d*] pyrimidine-6-carbonitrile (2).

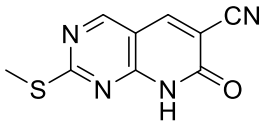

To a stirred solution of 4-amino-2-methylsulfanyl-pyrimidine-5-carbaldehyde (1) (10g, 59.2 mmol, 1.0 equiv.) in acetic acid (100 mL), was added cyanoacetic acid (6.05g, 71.1 mmol, 1.2 equiv.) and benzyl amine (634mg, 5.92mmol, 0.1 equiv.). The reaction mixture was allowed to stir at 100℃ for 6 h. Progress of the reaction was monitored by TLC and LCMS. After completion of the reaction, the reaction mixture was cooled to room temperature and the precipitated product was filtered to give the desired product without any further purification. Intermediate **2** was obtained as a yellow solid (8.64g) in 67% yield. LRMS (ESI^+): m/z calculated for $C_9H_7N_4OS^+$: 219.03 $[M+H]^+$; found 219.10. ^1H NMR (600 MHz, DMSO-d_6) δ 8.07 (s, 1H), 7.90 (s, 1H), 1.75 (s, 3H).

General procedure for the synthesis of intermediate 3.

To a stirred solution of intermediate **2** (2.19g, 10.0 mmol, 1.0 equiv.) in anhydrous DMF (30 mL) was added sodium hydride (60% dispersion in mineral oil, 600mg, 15.0 mmol, 1.5 equiv.) at room temperature. After stirring for 30 minutes, corresponding bromide (15.0 mmol) and KI (166mg, 1.0 mmol, 1.0 equiv.) was added. The reaction mixture was allowed to stir at room temperature for 12h. Progress of the reaction was monitored by TLC and LCMS. After completion of the reaction, the reaction mixture was cooled to 0℃ and quenched with cold water and extracted with EtOAc for three times. The combined organic layer was washed with water and brine, dried over anhydrous Na_2SO_4, filtered and concentrated under reduced pressure. The residue was purified by flash chromatography (DCM in MeOH, 0-10%) to give the desired product **3**.

***tert*-Butyl(2-(6-cyano-2-(methylthio)-7-oxopyrido[2,3-*d*]pyrimidin-8(7H)-yl)ethyl)carbamate (3a)**

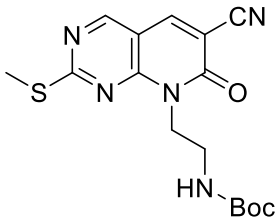

tert-Butyl (2-bromoethyl) carbamate was used, and **3a** was obtained as a yellow solid (1.92g) in 53% yield. LRMS (ESI^+): m/z calculated for $C_{16}H_{19}N_5O_3SNa^+$: 384.12 $[M+Na]^+$; found 384.11. ^1H NMR (600 MHz, Chloroform-*d*) δ 8.69 (s, 1H), 8.16 (s, 1H), 4.60 (s, 2H), 3.56 (q, *J* = 5.9 Hz, 2H), 2.65 (s, 3H), 1.32 (s, 9H).

***tert*-Butyl(3-(6-cyano-2-(methylthio)-7-oxopyrido[2,3-*d*]pyrimidin-8(7H)-yl)propyl)carbamate (3b)**

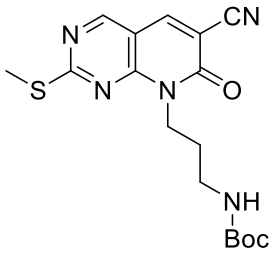

tert-Butyl (3-bromopropyl)carbamate was used, and **3b** was obtained as a yellow solid (1.90g) in 51% yield. LRMS (ESI^+): m/z calculated for $C_{17}H_{21}N_5O_3SNa^+$: 398.13 $[M+Na]^+$; found 398.11.

^{1}H NMR (600 MHz, Chloroform-*d*) δ 8.70 (s, 1H), 8.16 (s, 1H), 4.50 (t, *J* = 6.8 Hz, 2H), 3.14 (q, *J* = 6.3 Hz, 2H), 2.65 (s, 3H), 1.96 (p, *J* = 6.6 Hz, 2H), 1.44 (s, 9H).

General procedure for the synthesis of intermediate 4.

To a stirred solution of intermediate **3** (5.0 mmol, 1.0 equiv.) in CH_2Cl_2 (25 mL) was added *m*-CPBA (2.07g, 12 mmol, 2.4 equiv.) in one portion at 0℃. The reaction mixture was allowed to stir at room temperature for 1 h. Progress of the reaction was monitored by TLC and LCMS. After completion of the reaction, the reaction mixture was quenched with sodium bicarbonate solution and extracted with CH_2Cl_2 for three times. The combined organic layer was washed with water and brine, dried over anhydrous Na_2SO_4, filtered and concentrated under reduced pressure to obtain the desired product **4**, which was used for the next step without any further purification.

***tert*-Butyl(2-(6-cyano-2-(methylsulfonyl)-7-oxopyrido[2,3-*d*]pyrimidin-8(7H)-yl)ethyl)carbamate (4a)**

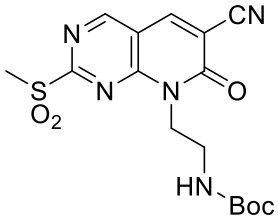

4a was obtained as a yellow solid (1.77g) in 90% yield. LRMS (ESI^+): m/z calculated for $C_{16}H_{20}N_5O_5S^+$: 394.11 $[M+H]^+$; found 394.11.

***tert*-Butyl(3-(6-cyano-2-(methylsulfonyl)-7-oxopyrido[2,3-*d*]pyrimidin-8(7H)-yl)propyl)carbamate (4b)**

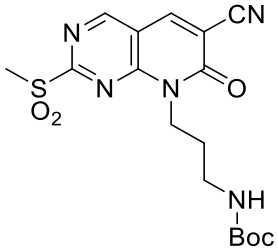

4b was obtained as a yellow solid (1.66g) in 82% yield. LRMS (ESI^+): m/z calculated for $C_{17}H_{22}N_5O_5S^+$: 408.12 $[M+H]^+$; found 408.11.

General procedure for the synthesis of intermediate 5.

To a stirred solution of substituted **4** (4.0 mmol, 1.0 equiv.) in DMF (20 mL) was added corresponding amine (6.0 mmol, 2.0 equiv.) and triethylamine (1.1ml, 8.0 mmol, 2.0 equiv.) at room temperature. The reaction mixture was allowed to stir at room temperature for 12 h. Progress of the reaction was monitored by TLC and LCMS. After completion of the reaction, the reaction mixture was quenched with water, extracted with EtOAc for three times. The combined organic layer was washed with water and brine, dried over anhydrous Na_2SO_4, filtered and concentrated under reduced pressure. The residue was purified by flash chromatography (DCM in MeOH, 0-10%) to give the desired product **5**.

***tert*-Butyl(2-(6-cyano-2-(methylamino)-7-oxopyrido[2,3-*d*]pyrimidin-8(7H)-yl)ethyl)carbamate (5a)**

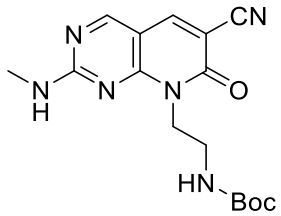

Methylamine hydrochloride and **4a** were used, and **5a** was obtained as a yellow solid (828mg) in 60% yield. LRMS (ESI^+): m/z calculated for $C_{16}H_{21}N_6O_3^+$: 345.16 $[M+H]^+$; found 345.17. ^1H NMR (500 MHz, DMSO-d_6) δ 8.66 (s, 1H), 8.50 (s, 1H), 4.24 (t, J = 7.3 Hz, 2H), 3.00 – 2.95 (m, 2H), 2.93 (dd, J = 4.9, 1.9 Hz, 3H), 1.36 (s, 9H).

***tert*-Butyl(3-(6-cyano-2-(methylamino)-7-oxopyrido[2,3-*d*]pyrimidin-8(7H)-yl)propyl)carbamate (5b)**

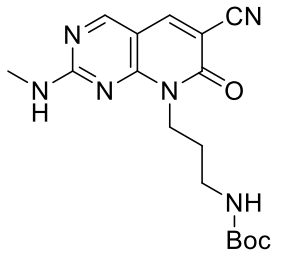

Methylamine hydrochloride and **4b** were used, and **5b** was obtained as a yellow solid (816mg) in 57% yield. LRMS (ESI^+): m/z calculated for $C_{17}H_{23}N_6O_3^+$: 359.18 $[M+H]^+$; found 359.17. ^1H

NMR (500 MHz, DMSO-d_6) δ 8.64 (s, 1H), 8.48 (s, 1H), 4.33 (t, *J* = 5.8 Hz, 2H), 3.28 – 3.25 (m, 2H), 2.94 (s, 2H), 2.92 (d, *J* = 7.7 Hz, 3H), 1.25 (s, 9H).

***tert*-Butyl(2-(6-cyano-2-((1-(methylsulfonyl)piperidin-4-yl)amino)-7-oxopyrido[2,3-*d*]pyrimidin-8(7H)-yl)ethyl)carbamate (5c)**

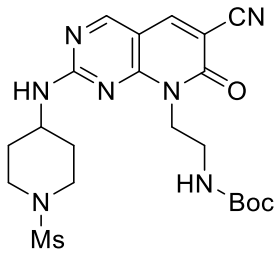

1-(Methylsulfonyl)-4-piperidinamine and **4a** were used, and **5c** was obtained as a yellow solid (1.28g) in 65% yield. LRMS (ESI$^+$): m/z calculated for $C_{21}H_{30}N_7O_5S^+$: 492.19 $[M+H]^+$; found 492.20. ^{1}H NMR (600 MHz,DMSO-d_6) δ 8.52 (d, *J* = 14.5 Hz, 1H), 8.00 (d, *J* = 7.2 Hz, 1H), 5.01 (s, 1H), 4.46 (q, *J* = 7.8, 7.3 Hz, 2H), 3.81 (d, *J* = 12.1 Hz, 2H), 3.56 - 3.41 (m, 2H), 2.82 (s, 3H), 2.19 (dd, *J* = 27.9, 11.9 Hz, 2H), 1.85 - 1.60 (m, 2H), 1.40 (s, 9H).

***tert*-Butyl(3-(6-cyano-2-((1-(methylsulfonyl)piperidin-4-yl)amino)-7-oxopyrido[2,3-*d*]pyrimidin-8(7H)-yl)propyl)carbamate (5d)**

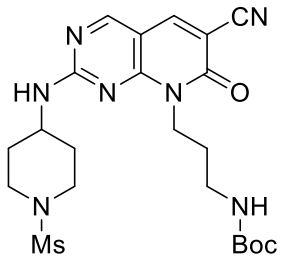

1-(Methylsulfonyl)-4-piperidinamine and **4b** were used, **5d** was obtained as a yellow solid (1.36g) in 67% yield. LRMS (ESI$^+$): m/z calculated for $C_{22}H_{32}N_7O_5S^+$: 506.21 $[M+H]^+$; found 506.20. ^{1}H NMR (600 MHz, Chloroform-*d*) δ 8.52 (d, *J* = 14.4 Hz, 1H), 7.99 (d, *J* = 10.2 Hz, 1H), 4.35 (d, *J* = 28.2 Hz, 2H), 3.82 (d, *J* = 12.4 Hz, 2H), 3.15 (t, *J* = 6.6 Hz, 2H), 2.98 (dt, *J* = 10.2, 6.4 Hz, 1H), 2.84 (d, *J* = 13.8 Hz, 3H), 2.20 (d, *J* = 13.4 Hz, 2H), 1.96 – 1.85 (m, 1H), 1.74 (d, *J* = 11.0 Hz, 4H), 1.43 (s, 9H).

General procedure for the synthesis of intermediate 6.

To a solution of **5** (2.0 mmol, 1.0 equiv.) in CH_2Cl_2 (10 mL) was added trifluoroacetic acid (5 mL). The reaction was stirred at room temperature for 12 h and monitored by LCMS. After completion of the reaction, the mixture was concentrated under reduced pressure to obtain desired product 6, which was used for the next step without any further purification.

8-(2-Aminoethyl)-2-(methylamino)-7-oxo-7,8-dihydropyrido[2,3-d]pyrimidine-6-carbonitrile (6a)

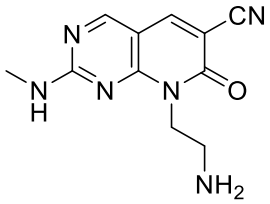

6a was obtained as a yellow solid (449mg) in 92% yield. LRMS (ESI^+): m/z calculated for $C_{11}H_{13}N_6O^+$: 245.16$[M+H]^+$; found 245.17.

8-(3-Aminopropyl)-2-(methylamino)-7-oxo-7,8-dihydropyrido[2,3-*d*]pyrimidine-6-carbonitrile (6b)

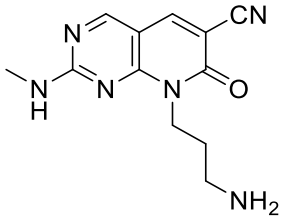

6b was obtained as a yellow solid (482mg) in 93% yield. LRMS (ESI^+): m/z calculated for $C_{12}H_{15}N_6O^+$: 259.13 $[M+H]^+$; found 259.17.

8-(2-Aminoethyl)-2-((1-(methylsulfonyl)piperidin-4-yl)amino)-7-oxo-7,8-dihydropyrido[2,3-*d*]pyrimidine-6-carbonitrile(6c)

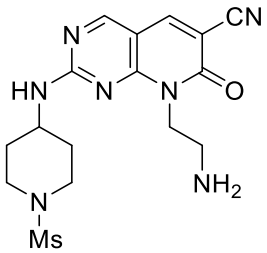

6c was obtained as a yellow solid (706mg) in 91% yield. LRMS (ESI^+): m/z calculated for $C_{16}H_{22}N_7O_3S^+$: 392.14 $[M+H]^+$; found 392.20. ^1H NMR (600 MHz, DMSO-d_6) δ 8.72 (s, 1H), 8.56 (d, *J* = 5.4 Hz, 1H), 4.44 (dt, *J* = 46.9, 5.7 Hz, 2H), 4.05 (dq, *J* = 10.4, 3.2 Hz, 1H), 3.62- 3.49 (m, 2H), 3.18 (p, *J* = 5.9, 5.0 Hz, 2H), 2.94 (td, *J* = 11.8, 2.8 Hz, 2H), 2.89 (s, 3H), 1.96 (dd, *J* = 11.2, 6.4 Hz, 2H), 1.70- 1.52 (m, 2H).

8-(3-Aminopropyl)-2-((1-(methylsulfonyl)piperidin-4-yl)amino)-7-oxo-7,8-dihydropyrido[2,3-*d*]pyrimidine-6-carbonitrile (6d)

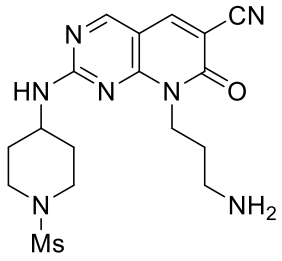

6d was obtained as a yellow solid (729mg) in 90% yield. LRMS (ESI^+): m/z calculated for $C_{17}H_{24}N_7O_3S^+$: 406.21 $[M+H]^+$; found 406.20. ^1H NMR (600 MHz, DMSO-d_6) δ 8.75 (d, *J* = 31.4 Hz, 1H), 8.56 (s, 1H), 4.26 (dt, *J* = 33.4, 6.6 Hz, 2H), 3.58 (dt, *J* = 8.1, 4.4 Hz, 2H), 2.93 (dd, *J* = 11.8, 2.9 Hz, 2H), 2.89 (d, *J* = 5.3 Hz, 3H), 2.88 – 2.77 (m, 2H), 2.04 – 1.89 (m, 4H), 1.69 – 1.55 (m, 2H).

General procedure for the synthesis of LL-DA-1~4.

To a solution of **6** (1.0 mmol, 1.0 equiv.) in DMF (5 mL) was added 1H-Pyrazole-1-carboxamidine hydrochloride (293mg, 2.0 mmol, 2.0 equiv.) and triethylamine (2 mmol) at room temperature. The mixture was kept at room temperature for 12 h. Progress of the reaction was monitored by TLC and LCMS. After completion of the reaction, the reaction mixture was quenched with water and extracted with CH_2Cl_2 for three times. The combined organic layer was washed with water and brine, dried over anhydrous Na_2SO_4, filtered and concentrated under reduced pressure. The residue was purified by semi-preparative HPLC to afford desired product **LL-DA-1~4**.

1-(2-(6-Cyano-2-(methylamino)-7-oxopyrido[2,3-*d*]pyrimidin-8(7H)-yl)ethyl)guanidine (LL-DA-1)

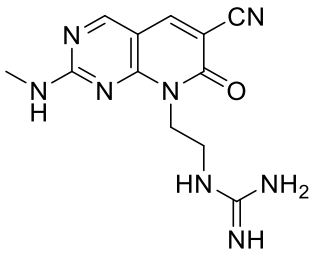

LL-DA-1 was obtained as a yellow solid (152mg) in 53% yield. HRMS (ESI^+): m/z calculated for $C_{12}H_{15}N_8O^+$: 287.1363 $[M+H]^+$; found 287.1364. Purity 98.30% (HPLC). ^1H NMR (500 MHz, DMSO-d_6) δ 8.64 (s, 1H), 8.51 (s, 1H), 8.41 (p, J = 6.1, 5.5 Hz, 2H), 8.33 – 8.29 (m, 1H), 4.38 (t, J = 5.6 Hz, 2H), 3.48 (q, J = 5.8 Hz, 2H), 2.92 (dd, J = 8.6, 4.7 Hz, 3H). ^{13}C NMR (126 MHz, DMSO-d_6) δ 163.00, 161.46, 160.82, 158.01, 157.04, 146.52, 116.88, 104.40, 98.11, 38.26, 28.51, 28.25. The value of absorption peak at 374 nm. The value of fluorescence emission peak at 409 nm. Cyclic voltammograms of LL-DA-1 in DMF with $E_{1/2}^{red}$ = -0.787 V (vs. Ag/AgCl).

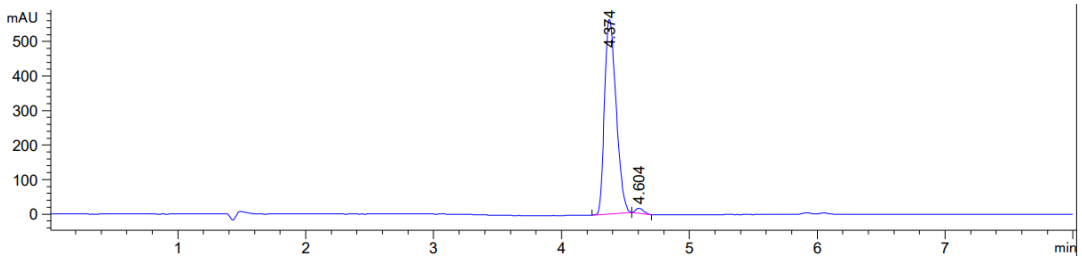

Signal 1: DAD1 B, Sig=254,4 Ref=off

Peak #	RetTime [min]	Type	Width [min]	Area [mAU*s]	Height [mAU]	Area %
1	4.374	BB	0.0997	3562.85718	564.34717	98.3014
2	4.604	BB	0.0697	61.56441	14.45192	1.6986
Totals :				3624.42159	578.79908	

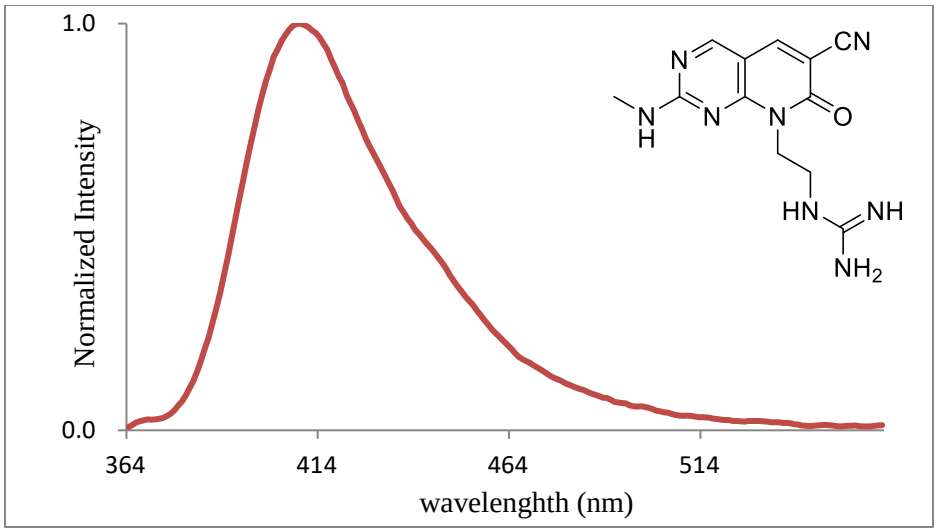
1.0
0.0
Normalized Intensity
364
414
464
514
wavelenghth (nm)
CN
N
N
H
N
N
O
HN
NH
NH2

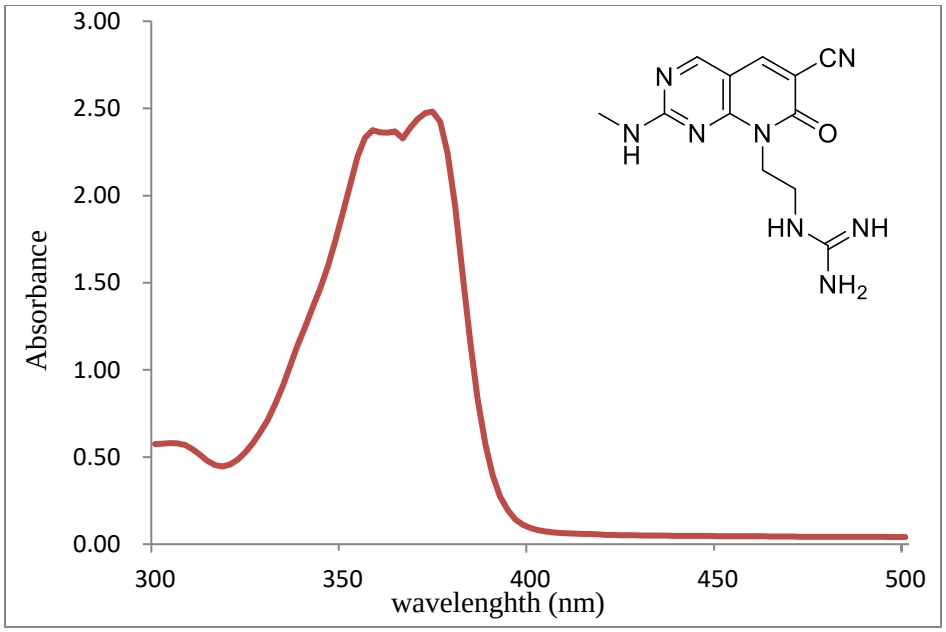
3.00
2.50
2.00
1.50
1.00
0.50
0.00
Absorbance
300
350
400
450
500
wavelenghth (nm)
CN
N
N
H
N
N
O
HN
NH
NH2

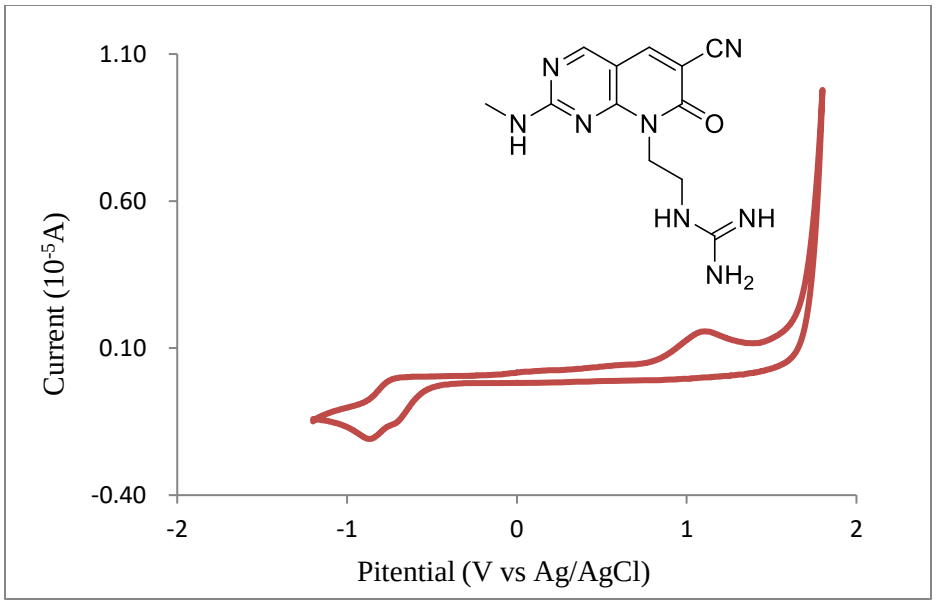

1-(3-(6-Cyano-2-(methylamino)-7-oxopyrido[2,3-*d*]pyrimidin-8(7H)-yl)propyl)guanidine (LL-DA-2)

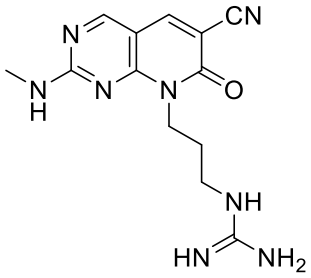

LL-DA-2 was obtained as a yellow solid (163mg) in 55% yield. HRMS (ESI^+): m/z calculated for $C_{13}H_{17}N_8O^+$: 301.1520 $[M+H]^+$; found 301.1517. Purity 97.43% (HPLC). ^{1}H NMR (500 MHz, DMSO-d_6) δ 8.65 (s, 1H), 8.50 (s, 1H), 4.24 (dt, *J* = 46.2, 6.9 Hz, 2H), 3.13 (dq, *J* = 18.8, 6.4 Hz, 2H), 2.93 (dd, *J* = 12.1, 4.7 Hz, 3H), 1.83 (dt, *J* = 19.9, 6.8 Hz, 2H). ^{13}C NMR (151 MHz, DMSO-d_6) δ 163.07, 161.57, 160.70, 157.86, 156.56, 146.41, 116.88, 104.35, 98.22, 39.02, 38.93, 28.42, 27.25. The value of absorption peak at 372 nm. The value of fluorescence emission peak at 408 nm. Cyclic voltammograms of LL-DA-2 in DMF with $E_{1/2}^{red}$ = -0.778V (vs. Ag/AgCl).

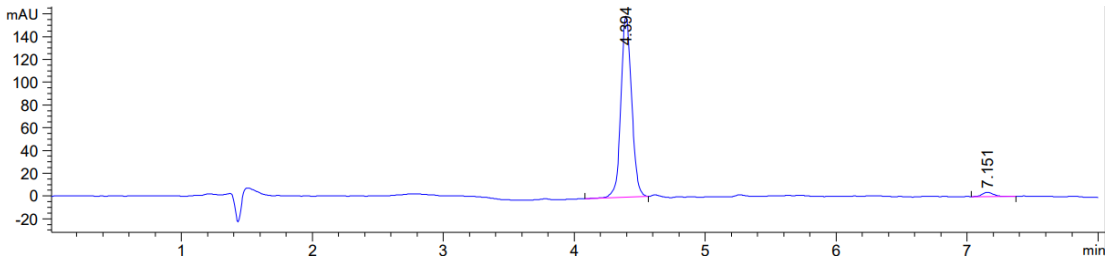

Signal 1: DAD1 B, Sig=254,4 Ref=off

Peak #	RetTime [min]	Type	Width [min]	Area [mAU*s]	Height [mAU]	Area %
1	4.394	BB	0.0886	905.43420	158.72069	97.4307
2	7.151	BB	0.0936	23.87652	3.78276	2.5693
Totals :				929.31072	162.50345	

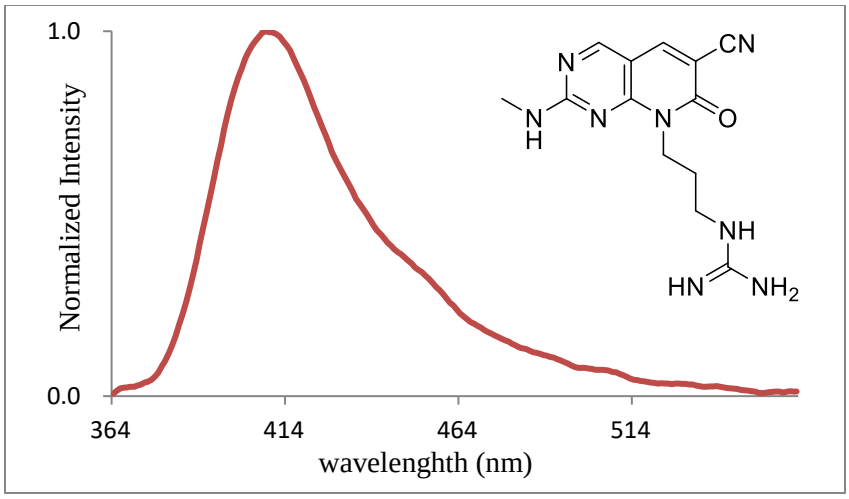

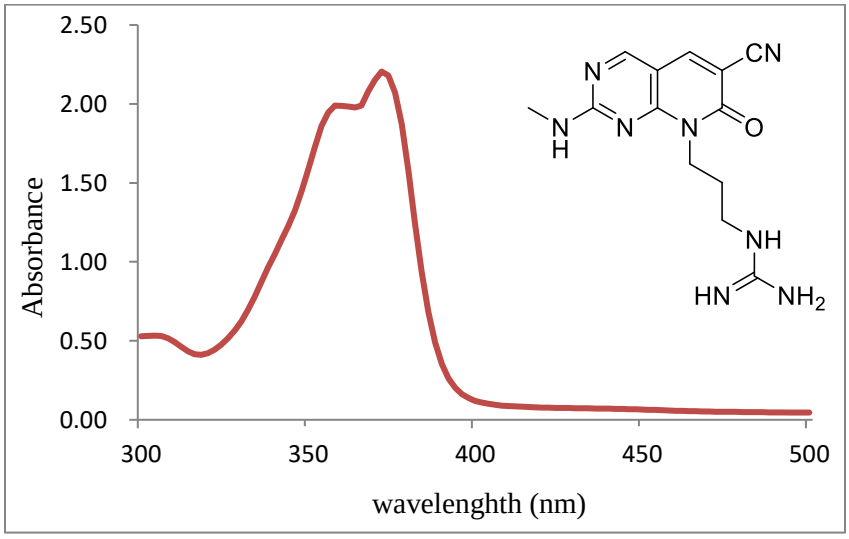

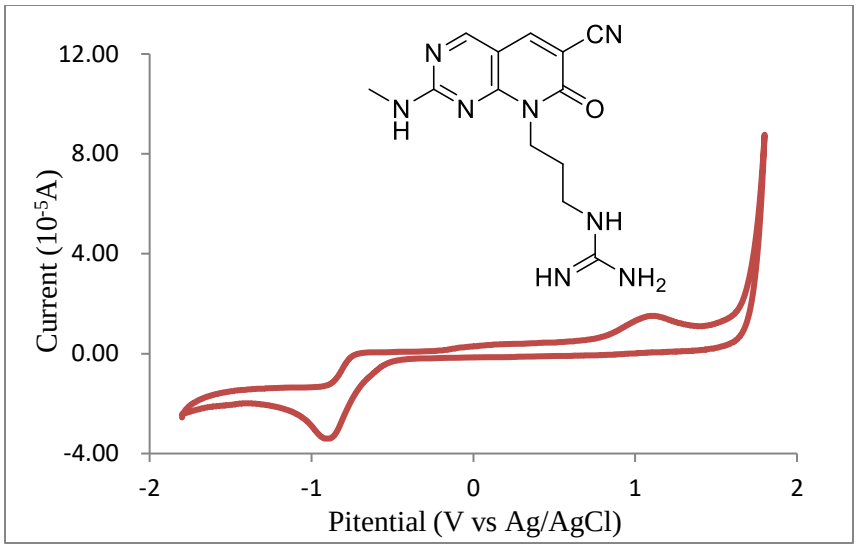

1-(2-(6-Cyano-2-((1-(methylsulfonyl)piperidin-4-yl)amino)-7-oxopyrido[2,3-*d*]pyrimidin-8(7H)-yl)ethyl)guanidine (LL-DA-3)

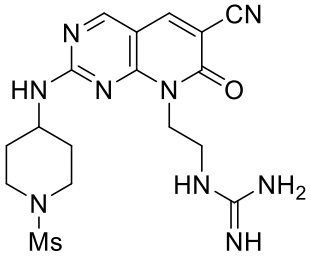

LL-DA-3 was obtained as a yellow solid (232mg) in 54% yield. HRMS (ESI^+): m/z calculated for $C_{17}H_{24}N_9O_3S^+$: 434.1717 $[M+H]^+$; found 434.1718. Purity 99.63% (HPLC). ^1H NMR (600 MHz, DMSO-d_6) δ 8.67 (s, 1H), 8.51 (s, 1H), 4.30 (dt, *J* = 28.6, 5.5 Hz, 2H), 3.90 (ddt, *J* = 14.4, 10.6, 5.3 Hz, 1H), 3.62 - 3.50 (m, 2H), 3.48 (q, *J* = 5.9 Hz, 2H), 2.85 (s, 3H), 2.46 (q, *J* = 1.9 Hz, 2H), 2.00 - 1.82 (m, 2H), 1.55 (tdd, *J* = 14.8, 10.2, 3.8 Hz, 2H). ^{13}C NMR (126 MHz, DMSO-d_6) δ 163.47, 161.91, 161.66, 160.74, 157.60, 156.97, 116.75, 104.68, 98.59, 47.98, 45.02, 44.88, 38.50, 34.96, 30.75. The value of absorption peak at 374 nm. The value of fluorescence emission peak at 410 nm. Cyclic voltammograms of LL-DA-3 in DMF with $E_{1/2}^{red}$ = -0.728V (vs. Ag/AgCl).

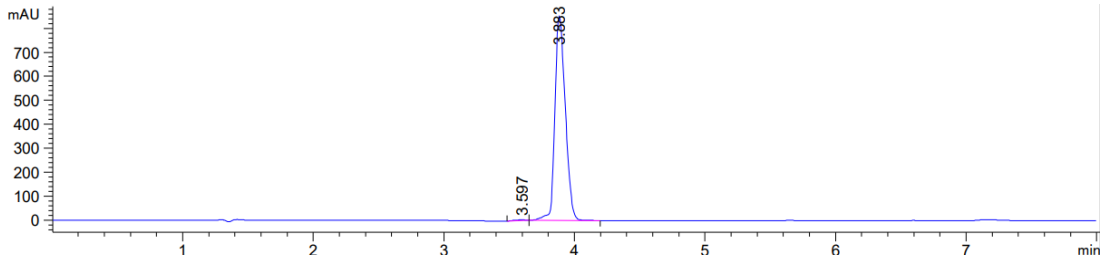

Signal 1: DAD1 B, Sig=254,4 Ref=off

Peak #	RetTime [min]	Type	Width [min]	Area [mAU*s]	Height [mAU]	Area %
1	3.597	BB	0.0682	17.35111	3.59969	0.3649
2	3.883	BB	0.0850	4737.04053	850.11047	99.6351
Totals :				4754.39163	853.71017	

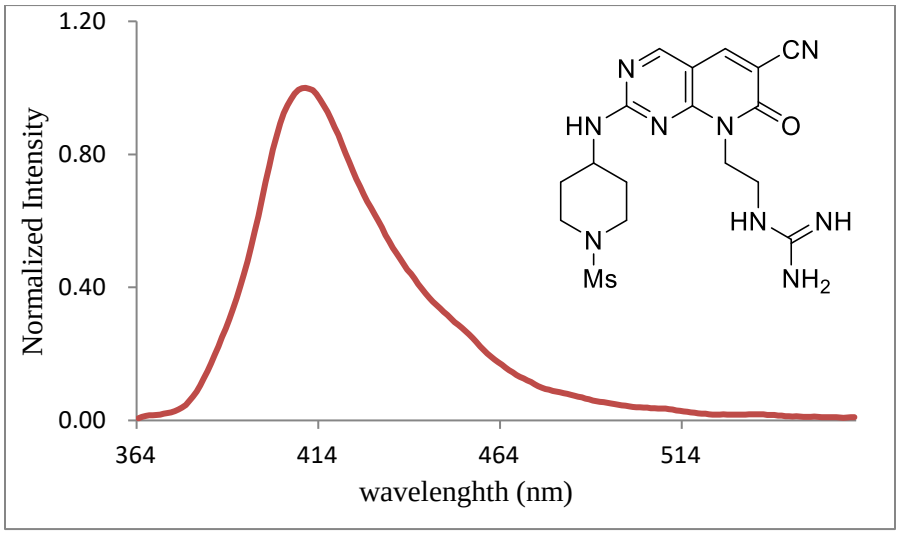

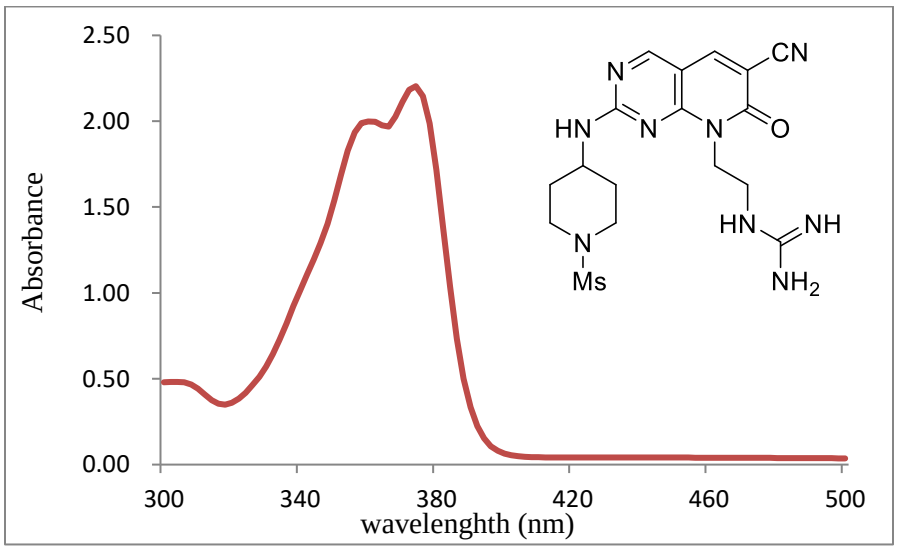

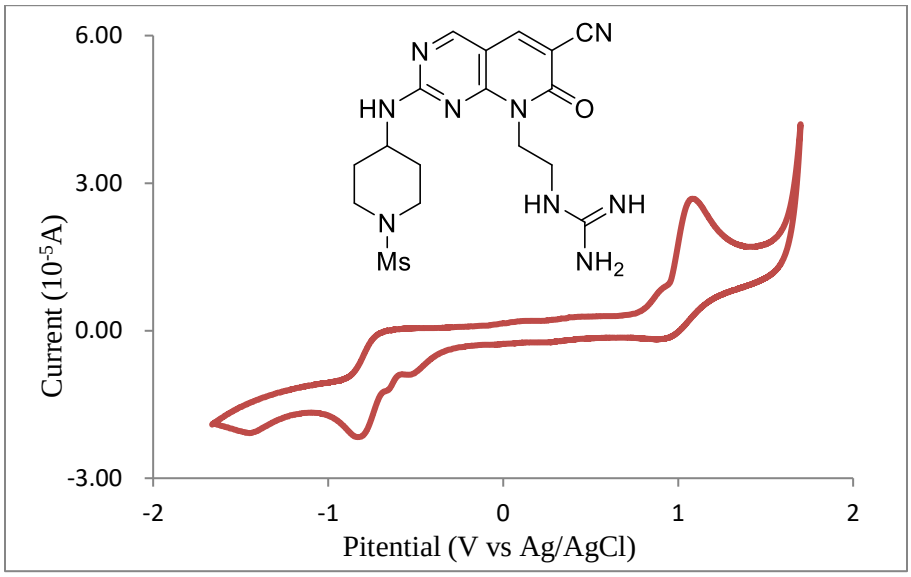

1-(3-(6-cyano-2-((1-(methylsulfonyl)piperidin-4-yl)amino)-7-oxopyrido[2,3-d]pyrimidin-8(7H)-yl)propyl)guanidine (LL-DA-4)

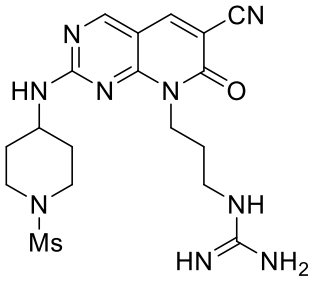

LL-DA-4 was obtained as a yellow solid (242mg) in 54% yield. HRMS (ESI^+): m/z calculated for $C_{17}H_{25}N_{10}O_3S^+$: 448.1874 $[M+H]^+$; found 448.1874. Purity 97.74% (HPLC). ^1H NMR (600 MHz, DMSO-d_6) δ 8.74 (d, *J* = 30.2 Hz, 1H), 8.54 (d, *J* = 1.3 Hz, 1H), 4.25 (dt, *J* = 31.5, 6.7 Hz, 2H), 3.97 (qd, *J* = 8.9, 7.6, 5.2 Hz, 1H), 3.55 (dt, *J* = 12.5, 4.3 Hz, 2H), 3.15 (dq, *J* = 12.0, 6.4 Hz, 2H), 2.95 - 2.90 (m, 2H), 2.89 (d, *J* = 3.8 Hz, 3H), 1.98 (td, *J* = 12.7, 6.2 Hz, 2H), 1.90 - 1.80 (m, 2H), 1.68 - 1.51 (m, 2H). ^{13}C NMR (151 MHz, DMSO-d_6) δ 162.01, 161.92, 160.87, 159.06, 157.32, 146.54, 116.88, 104.79, 98.69, 47.90, 44.64, 34.88, 31.24, 30.75, 27.48. The value of absorption peak at 374 nm. The value of fluorescence emission peak at 410 nm. Cyclic voltammograms of LL-DA-4 in DMF with $E_{1/2}^{red}$ = -0.757 V (vs. Ag/AgCl).

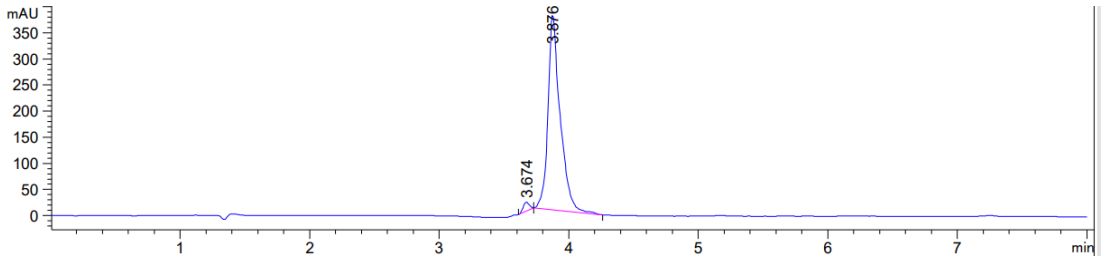

Signal 1: DAD1 B, Sig=254,4 Ref=off

Peak #	RetTime [min]	Type	Width [min]	Area [mAU*s]	Height [mAU]	Area %
1	3.674	BB	0.0552	56.31912	16.75834	2.2593
2	3.876	BB	0.0902	2436.43213	373.24997	97.7407
Totals :				2492.75125	390.00831	

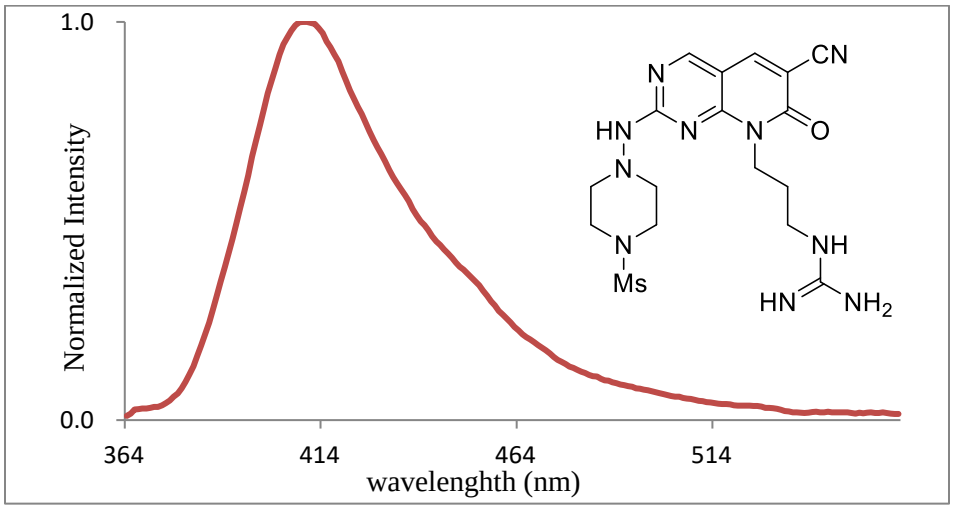

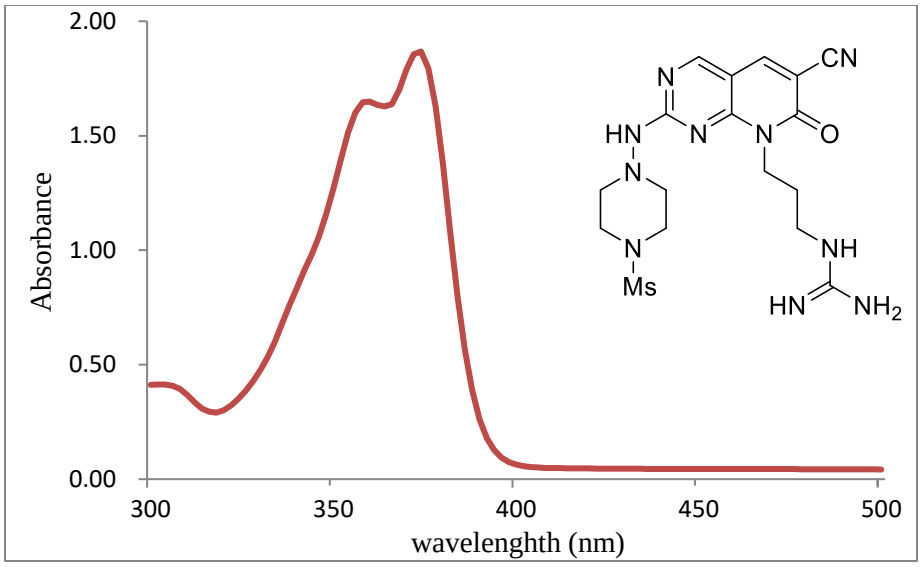
2.00
1.50
1.00
0.50
0.00
Absorbance
300
350
400
450
500
wavelenghth (nm)
CN
N
HN
N
N
N
O
N
Ms
NH
HN
NH2

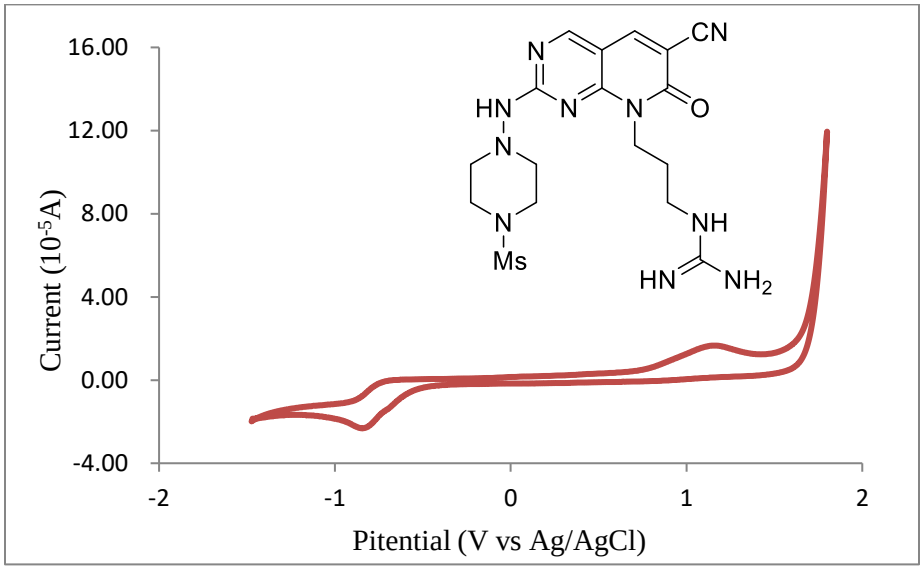
16.00
12.00
8.00
4.00
0.00
-4.00
Current (10-5A)
-2
-1
0
1
2
Pitential (V vs Ag/AgCl)
CN
N
HN
N
N
N
O
N
Ms
NH
HN
NH2

Scheme 2. Synthesis of PC-4

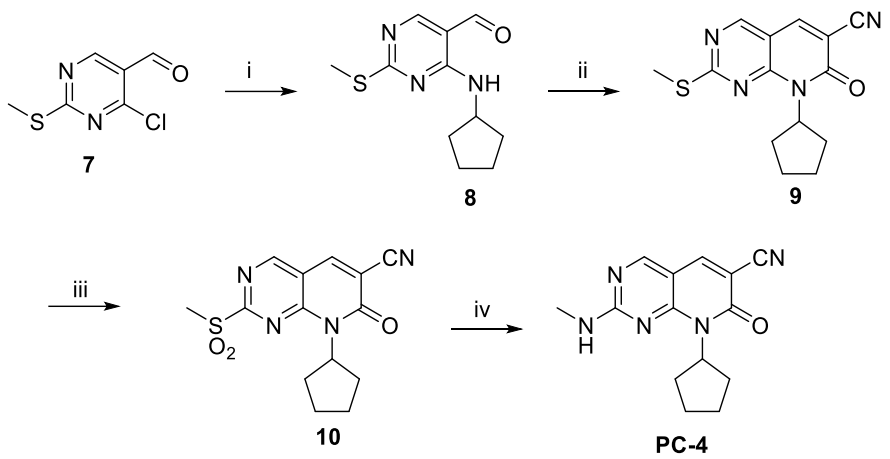

Reagents and conditions: (i) cyclopentylamine, TEA, CH_3CN, r.t.; (ii) $CNCH_2CO_2H$, $BnNH_2$, AcOH, 100°C; (iii) *m*-CPBA, CH_2Cl_2, 0°C-r.t.; (iv) methylamine hydrochloride, DMF, TEA, r.t..

4-(Cyclopentylamino)-2-(methylthio) pyrimidine-5-carbaldehyde (8)

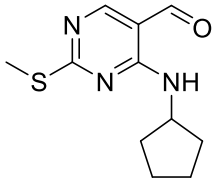

To a solution of 4-chloro-2-(methylthio) pyrimidine-5-carbaldehyde (**7**) (10g, 53.2 mmol, 1.0 equiv.) in CH_3CN (200 mL) was added cyclopentylamine (9.05g, 106.4 mmol, 2.0 equiv.), and triethylamine (14.8ml, 106.4 mmol, 2.0 equiv.) at room temperature and stirred for 12 h. Progress of the reaction was monitored by TLC and LCMS. After completion of the reaction, the mixture was quenched with water and extracted with EtOAc three times. The combined organic phases were washed with brine and dried over anhydrous Na_2SO_4, filtered and concentrated under reduced pressure. The residue was purified by flash chromatography (PE in EA, 0-100%) to give the desired product **8** as a white solid (11.3g) in 90% yield. LRMS (ESI^+): m/z calculated for $C_{11}H_{16}N_3OS^+$: 238.09 $[M+H]^+$; found 238.10. ^1H NMR (600 MHz, Chloroform-*d*) δ 9.85 (s, 1H), δ 7.58 (s, 1H), 4.46 (s, 2H), 4.41 (q, *J* = 6.8 Hz, 1H), 2.49 (s, 2H), 2.11 – 2.03 (m, 2H), 1.77 – 1.58 (m, 4H), 1.48 (dtd, *J* = 12.4, 8.0, 6.2 Hz, 2H).

8-Cyclopentyl-2-(methylthio)-7-oxo-7,8-dihydropyrido[2,3-*d*]pyrimidine-6-carbonitrile (9)

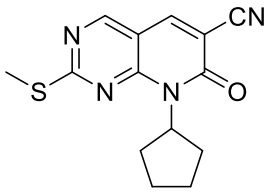

This compound was synthesized from **8** according to the methodology for the synthesis of intermediate **2**. Intermediate **9** was obtained as a yellow solid (1.52g) in 53% yield. LRMS (ESI^+): m/z calculated for $C_{14}H_{15}N_4OS^+$: 287.09 $[M+H]^+$; found 287.10. ^1H NMR (600 MHz, Chloroform-*d*) δ 8.68 (s, 1H), 8.10 (s, 1H), 5.94 (t, *J* = 8.8 Hz, 1H), 2.64 (s, 3H), 2.28 (dq, *J* = 14.6, 7.7 Hz, 2H), 2.09 (dq, *J* = 13.4, 7.7, 6.8 Hz, 2H), 1.91 (dq, *J* = 11.6, 6.9, 6.1 Hz, 2H), 1.78 – 1.61 (m, 3H).

8-Cyclopentyl-2-(methylsulfonyl)-7-oxo-7,8-dihydropyrido[2,3-*d*]pyrimidine-6-carbonitrile (10)

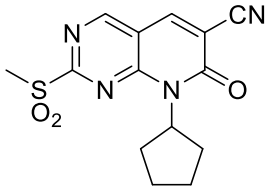

This compound was synthesized from **9** according to the methodology for the synthesis of intermediate **4**. Intermediate **10** was obtained as a yellow solid (1.42g) in 90% yield. LRMS (ESI^+): m/z calculated for $C_{14}H_{15}N_4O_3S^+$: 319.08 $[M+H]^+$; found 319.10.

8-Cyclopentyl-2-(methylamino)-7-oxo-7,8-dihydropyrido[2,3-*d*]pyrimidine-6-carbonitrile (PC-4)

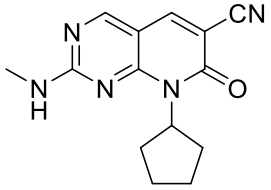

PC-4 was obtained according to the methodology for the synthesis of intermediate **5** as a yellow solid (637mg) in 60% yield. HRMS (ESI^+): m/z calculated for $C_{14}H_{16}N_5O^+$: 270.1349 $[M+H]^+$; found 270.1348. Purity 98.56% (HPLC). ^1H NMR (500 MHz, DMSO-d_6) δ 8.69 (d, *J* = 48.7 Hz, 1H), 8.47 (d, *J* = 4.3 Hz, 1H), 5.82 (dt, *J* = 20.6, 8.8 Hz, 1H), 2.92 (dd, *J* = 4.9, 3.2 Hz, 3H), 2.38 – 2.11 (m, 2H), 1.97 (td, *J* = 11.5, 6.2 Hz, 2H), 1.78 (ddd, *J* = 18.6, 10.7, 5.2 Hz, 2H), 1.70 – 1.51 (m, 2H). ^{13}C NMR (151 MHz, DMSO-d_6) δ 162.71 (d, *J* = 23.2 Hz), 162.34, 161.81, 160.77 (d, *J*

= 30.9 Hz), 156.89 (d, *J* = 54.0 Hz), 146.30 (d, *J* = 20.8 Hz), 116.80 (d, *J* = 16.1 Hz), 104.84 (d, *J* = 90.4 Hz), 99.27 (d, *J* = 87.3 Hz), 53.30 (d, *J* = 67.1 Hz), 28.59, 28.53, 28.10, 27.85, 25.99, 25.77. The value of absorption peak at 372 nm. The value of fluorescence emission peak at 408 nm. Cyclic voltammograms of PC-4 in DMF with $E_{1/2}^{red}$ = -0.775V (vs. Ag/AgCl)

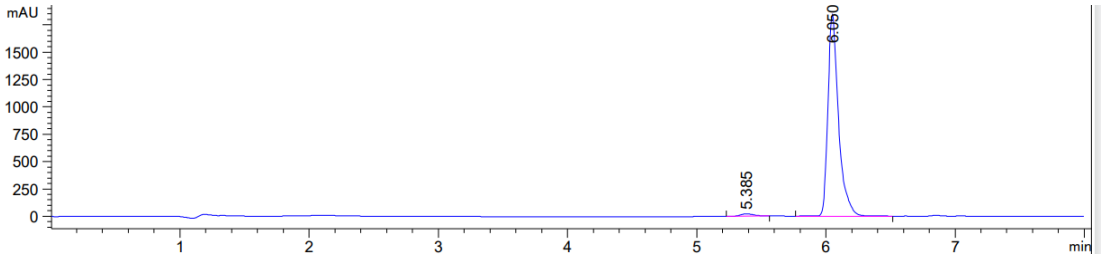

Signal 1: DAD1 B, Sig=254,4 Ref=off

Peak #	RetTime [min]	Type	Width [min]	Area [mAU*s]	Height [mAU]	Area %
1	5.385	BB	0.1081	153.05780	21.74500	1.4319
2	6.050	BB	0.0847	1.05361e4	1843.07446	98.5681
Totals :				1.06892e4	1864.81946	

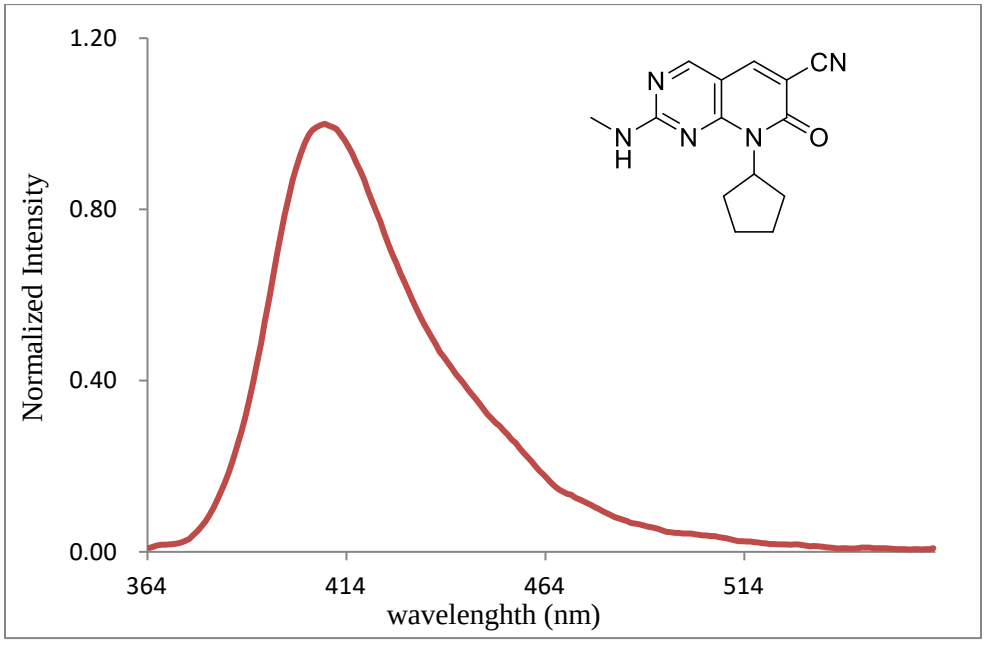

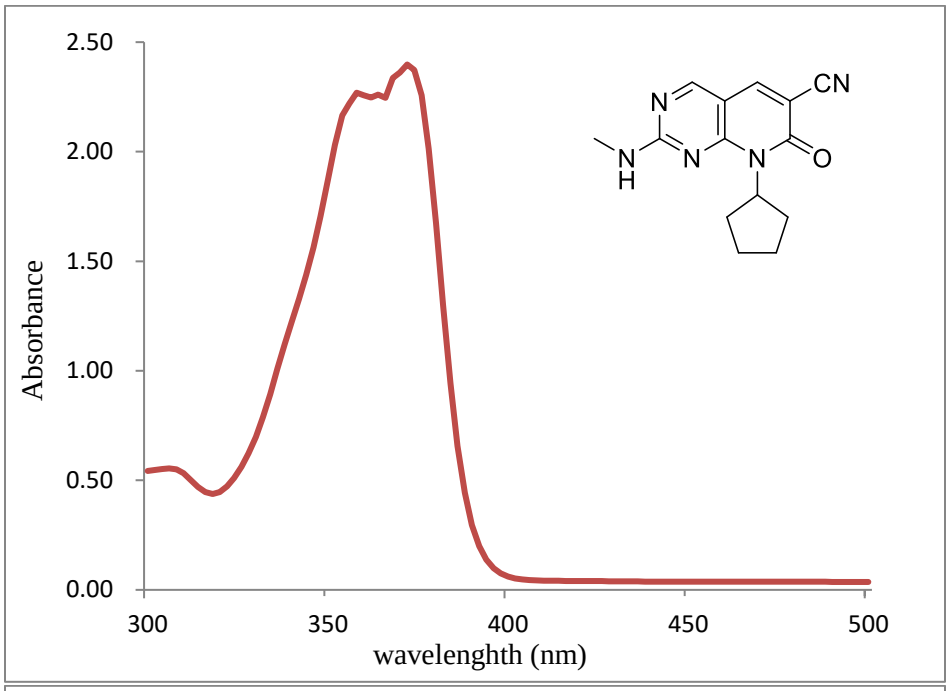
2.50
2.00
1.50
1.00
0.50
0.00
Absorbance
300
350
400
450
500
wavelenghth (nm)
CN
N
N
H
N
N
O

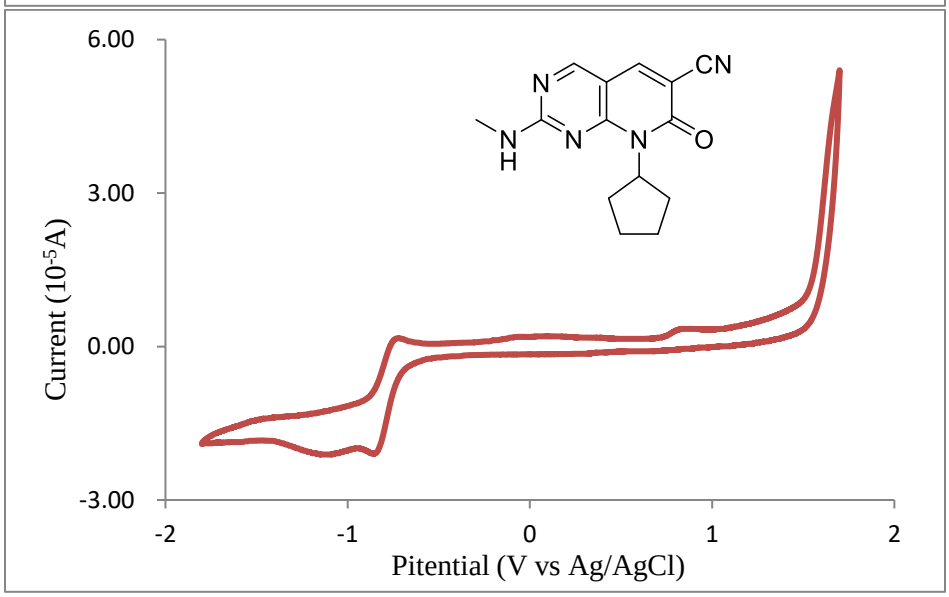
6.00
3.00
0.00
-3.00
Current (10-5A)
-2
-1
0
1
2
Pitential (V vs Ag/AgCl)
CN
N
N
H
N
N
O

Scheme 3. Synthesis of (*S*)-3-((((9*H*-fluoren-9-yl)methoxy)carbonyl)amino)-4-(methylamino)-4-oxobutanoic acid (a1)

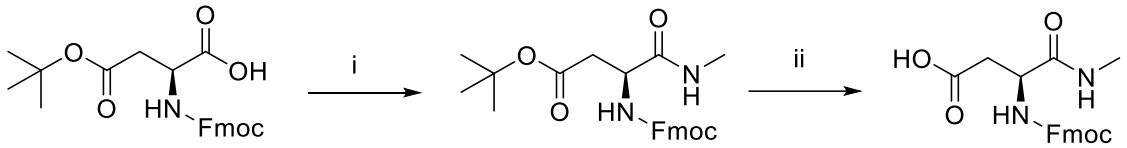

Reagents and conditions: (i) $CH_3NH_2 \cdot HCl$, HBTU, DIPEA, CH_2Cl_2, r.t.; (ii) TFA, CH_2Cl_2, r.t..

(*S*)-2-((((9H-fluoren-9-yl)methoxy)carbonyl)amino)-4-(tert-butoxy)-4-oxobutanoic acid (0.411g, 1 mmol, 1.0 equiv.) was dissolved in CH_2Cl_2 (20 mL). The Methylamine hydrochloride (0.167g, 2.5 mmol, 2.5 equiv.), HBTU (0.379 g, 1.00 mmol, 1.0 equiv.) and DIPEA (0.35 mL, 2.00 mmol, 2.0 equiv.) were then added to the reaction mixture, which was stirred at room temperature for 12 h. After reaction, the solution was washed with 1 M HCl (20 mL) and sat. $NaHCO_3$ (3 x 20 mL). The organic layers were then dried ($MgSO_4$) and concentrated *in vacuo*. The resulting crude solid was purified by column chromatography on silica gel using a gradient of methanol in DCM (0-20 %) as the eluent to give the desired amide product as a colorless liquid (0.27 g) in 64% yield.

The above amide was dissolved in CH_2Cl_2 (20 mL) followed by addition of TFA (5 mmol, 0.4 mL). Then the subsequent was stirring at room temperature for 2 h. After reaction, solvent removal under vacuum afforded a crude solid, which was purified by column chromatography on silica gel using a gradient of methanol in DCM (0-20 %) as the eluent to give the desired product **a1** as a white solid (0.21 g) in 90% yield. LRMS (ESI^+): m/z calculated for $C_{20}H_{21}N_2O_5^+$: 369.14 $[M+H]^+$; found 369.12. ^1H NMR (600 MHz, DMSO-*d*) δ 7.89 (d, *J* = 7.3 Hz, 2H), 7.80 (s, 1H), 7.72 (d, *J* = 7.1 Hz, 2H), 7.61 (d, *J* = 7.9 Hz, 1H), 7.42 (t, *J* = 7.2 Hz, 2H), 7.32 (d, *J* = 7.3 Hz, 2H), 4.30 (t, *J* = 8.4 Hz, 2H), 4.25 – 4.19 (m, 2H), 2.61 – 2.67 (m, 1H), 2.57 (d, *J* = 3.3 Hz, 3H), 2.46 - 2.47 (m, 1H).

Scheme 4. Synthesis of (9*H*-fluoren-9-yl)methyl (*S*)-(1-(methylamino)-1-oxopropan-2-yl)carbamate (b1)

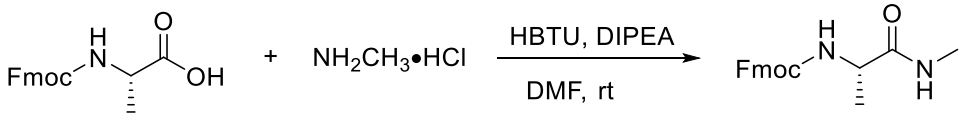

The (((9H-fluoren-9-yl)methoxy)carbonyl)-*L*-alanine (0.311g, 1 mmol, 1.0 equiv.) was dissolved in DMF (20 mL). The Methylamine hydrochloride (0.167g, 2.5 mmol, 2.5 equiv.), HBTU (0.380 g, 1.00 mmol, 1.0 equiv.) and DIPEA (0.35 mL, 2.00 mmol, 2.0 equiv.) were then added to the reaction mixture, which was stirred at room temperature for 12 h. After reaction, the solution was washed with 1 M HCl (20 mL) and sat. $NaHCO_3$ (3 x 20 mL). The organic layers were then dried ($MgSO_4$) and concentrated *in vacuo*. The resulting crude solid was purified by column chromatography on silica gel using a gradient of methanol in DCM (0-10 %) as the eluent to give the desired product **b1** a white solid (0.23 g) in 71.3 % yield. LRMS (ESI^+): m/z calculated for $C_{19}H_{21}N_2O_3^+$: 325.15 $[M+H]^+$; found 325.13. ^1H NMR (600 MHz, DMSO-*d*) δ 7.89 (d, *J* = 7.3 Hz, 2H), 7.80 (s, 1H), 7.72 (d, *J* = 7.1 Hz, 2H), 7.47 - 7.49 (m, 1H), 7.40 – 7.42 (m, 2H), 7.31 – 7.34 (m, 1H), 4.20 – 4.26 (m, 1H), 3.96 – 3.99 (m, 1H), 2.57 - 2.61 (m, 3H), 1.19 (d, *J* = 7.7 Hz, 3H).

Scheme 5. Synthesis of (*S*)-3-((((*9*H-fluoren-9-yl)methoxy)carbonyl)amino)-4-(((*S*)-1-methoxy-1-oxo-3-phenylpropan-2-yl)amino)-4-oxobutanoic acid (a2)

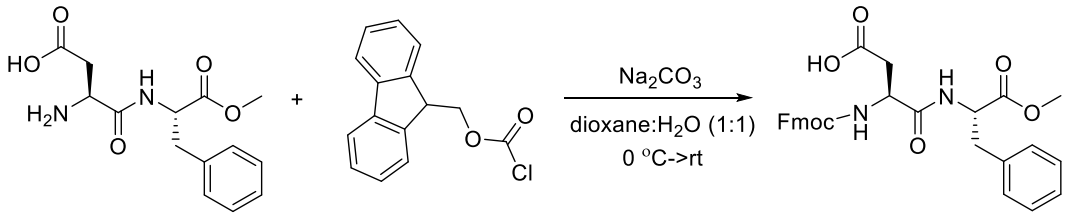

The Aspartame (0.294 g, 1.0 mmol, 1.0 equiv.) and Na_2CO_3 (0.16 g, 1.5 mmol, 1.5 equiv.) was dissolved in solvent mixture (dioxane: H_2O = 1: 1, 20 mL). The reaction was allowed to cool down to 0 °C and then Fmoc-Cl (0.31 g, 1.2 mmol, 1.2 equiv., in 10 mL dioxane) was dropwise added. The mixture was stirred at room temperature for 2 hours. After reaction, solvent removal under vacuum afforded a crude solid, which was purified by column chromatography on silica gel using a gradient of methanol in DCM (0-10 %) as the eluent to give the desired product a2 as a white solid. (0.25 g) in 49.5 % yield. LRMS (ESI^+): m/z calculated for $C_{29}H_{29}N_2O_7^+$: 517.19 $[M+H]^+$; found 517.17. ^1H NMR (600 MHz, DMSO-*d*) δ 8.29 (d, *J* = 7.6 Hz, 1H), 7.90 (d, *J* = 7.6 Hz, 2H), 7.74 – 7.68 (m, 2H), 7.62 (d, *J* = 8.2 Hz, 1H), 7.42 (t, *J* = 7.5 Hz, 2H), 7.33 (td, *J* = 7.3, 3.0 Hz,

2H), 7.24 (dd, *J* = 11.6, 7.0 Hz, 2H), 7.20 – 7.16 (m, 3H), 4.44 (dd, *J* = 13.9, 7.7 Hz, 1H), 4.38 (td, *J* = 9.0, 4.2 Hz, 1H), 4.19 - 4.22 (m, 2H), 4.05 (t, *J* = 6.2 Hz, 1H), 3.57 (s, 3H), 3.00 (dd, *J* = 13.7, 5.7 Hz, 1H), 2.96 – 2.92 (m, 1H), 2.61 (dd, *J* = 16.7, 4.2 Hz, 1H), 2.49 – 2.42 (m, 1H).

Scheme 6. Synthesis of methyl (((9*H*-fluoren-9-yl)methoxy)carbonyl)-*L*-alanyl-*L*-phenylalaninate (b2)

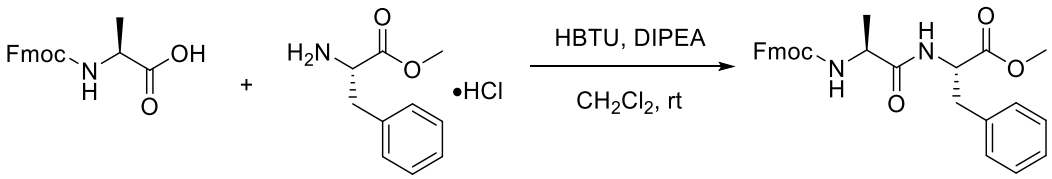

The methyl *L*-phenylalaninate hydrochloride (0.537g, 2.5 mmol, 2.5 equiv.) was dissolved in CH_2Cl_2 (20 mL). The (((9H-fluoren-9-yl)methoxy)carbonyl)-*L*-alanine (0.311g, 1.0 mmol, 1.0 equiv.), HBTU (0.379 g, 1.0 mmol, 1.0 equiv.) and DIPEA (0.35 mL, 2.0 mmol, 1.0 equiv.) were then added to the reaction mixture, which was stirred for 12 h. After reaction, the solution was washed with 1 M HCl (20 mL), sat. $NaHCO_3$ (3 x 20 mL) and H_2O (20 mL). The organic layers were then dried ($MgSO_4$) and concentrated to dryness *in vacuo*. The resulting crude solid was purified by column chromatography on silica gel using a gradient of methanol in DCM (0-10 %) as the eluent to give the desired product b2 as a white solid. (0.24 g) in 51.2 % yield. LRMS (ESI^+): m/z calculated for $C_{28}H_{29}N_2O_5^+$: 472.20 $[M+H]^+$; found 473.19. ^1H NMR (600 MHz, DMSO-*d*) δ 8.26 (d, *J* = 7.5 Hz, 1H), 7.89 (d, *J* = 7.5 Hz, 2H), 7.72 (t, *J* = 7.4 Hz, 2H), 7.46 (d, *J* = 7.8 Hz, 1H), 7.42 (t, *J* = 7.4 Hz, 2H), 7.32 (t, *J* = 7.4 Hz, 2H), 7.25 (t, *J* = 7.4 Hz, 2H), 7.19 (dd, *J* = 12.7, 7.1 Hz, 3H), 4.46 (dd, *J* = 14.1, 7.7 Hz, 1H), 4.25 (dd, *J* = 14.4, 6.8 Hz, 2H), 4.20 (dd, *J* = 14.0, 7.1 Hz, 1H), 4.11 – 4.05 (m, 1H), 3.57 (s, 3H), 3.01 (dd, *J* = 13.8, 5.9 Hz, 1H), 2.94 (dd, *J* = 13.7, 8.6 Hz, 1H), 1.18 (d, *J* = 7.1 Hz, 3H).

NMR spectra of tested compounds

1-(2-(6-Cyano-2-(methylamino)-7-oxopyrido[2,3-*d*]pyrimidin-8(7H)-yl)ethyl)guanidine (**LL-DA-1**)

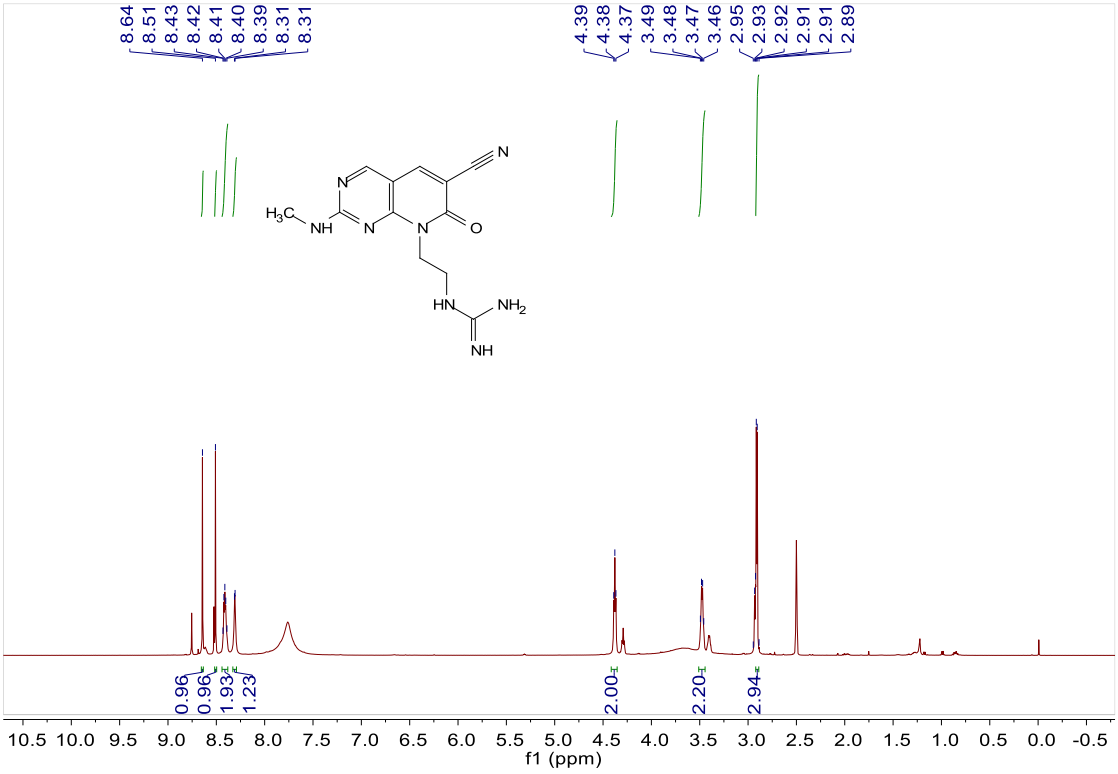

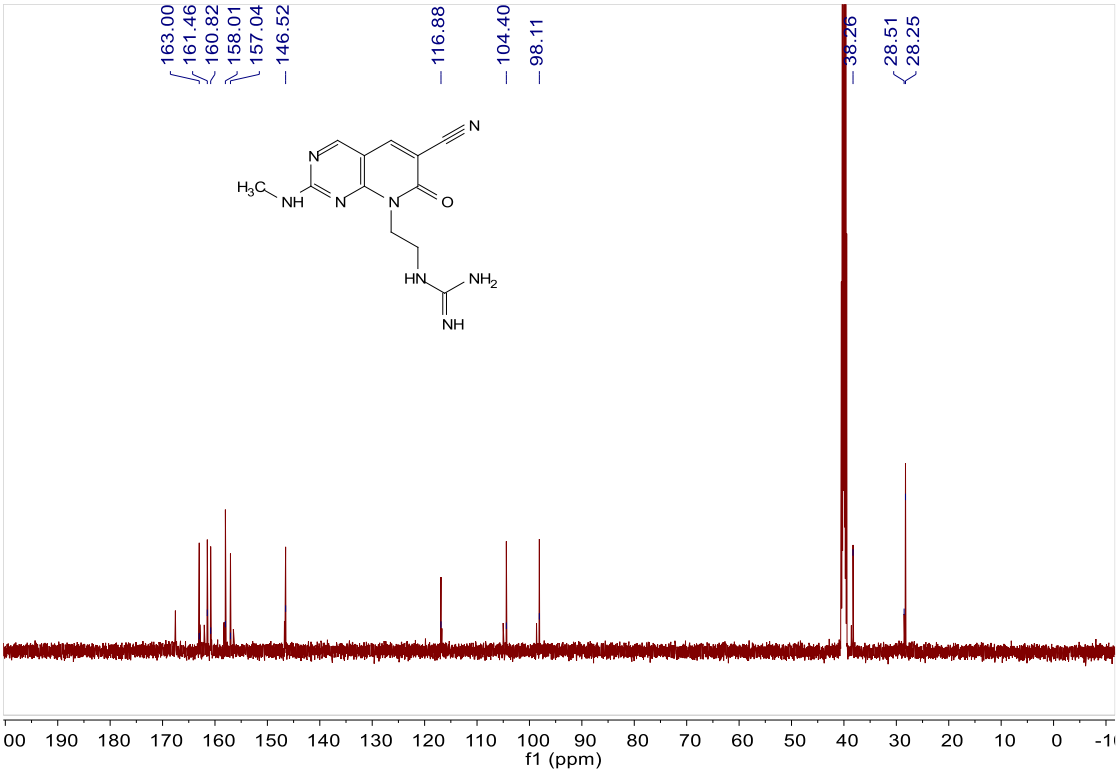

1-(3-(6-Cyano-2-(methylamino)-7-oxopyrido[2,3-*d*]pyrimidin-8(7H)-yl)propyl)guanidine (**LL-DA-2**)

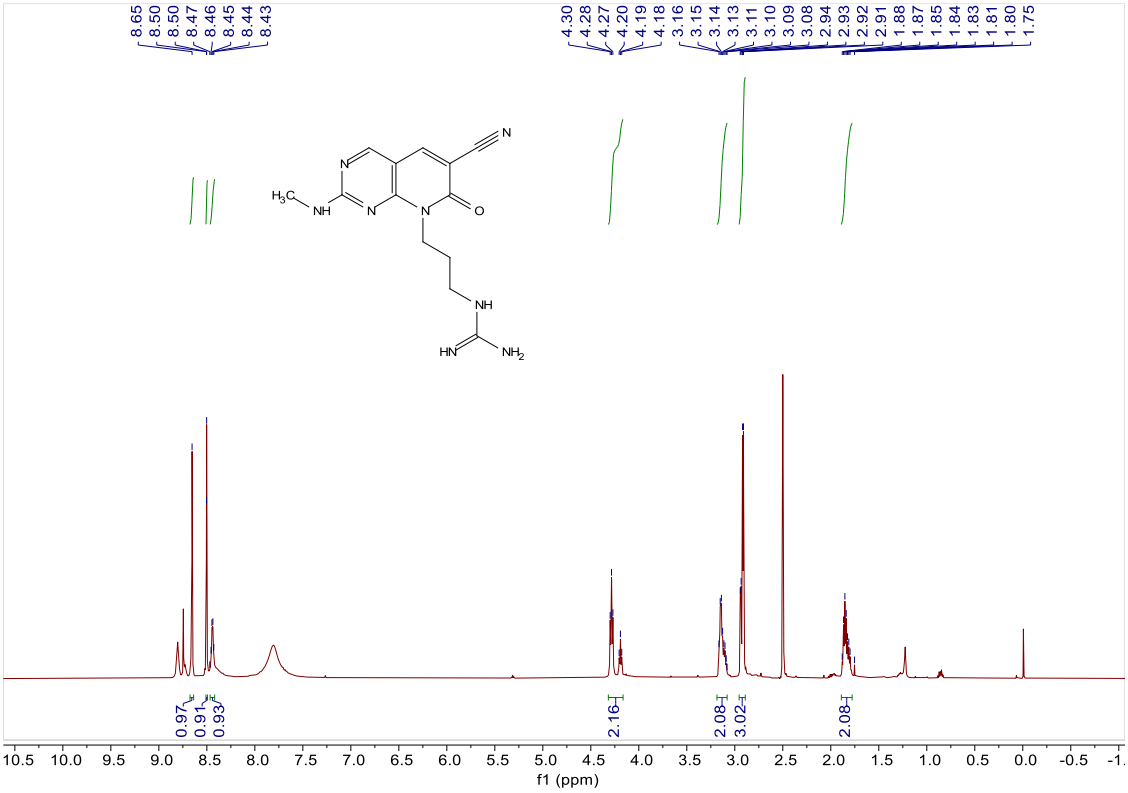

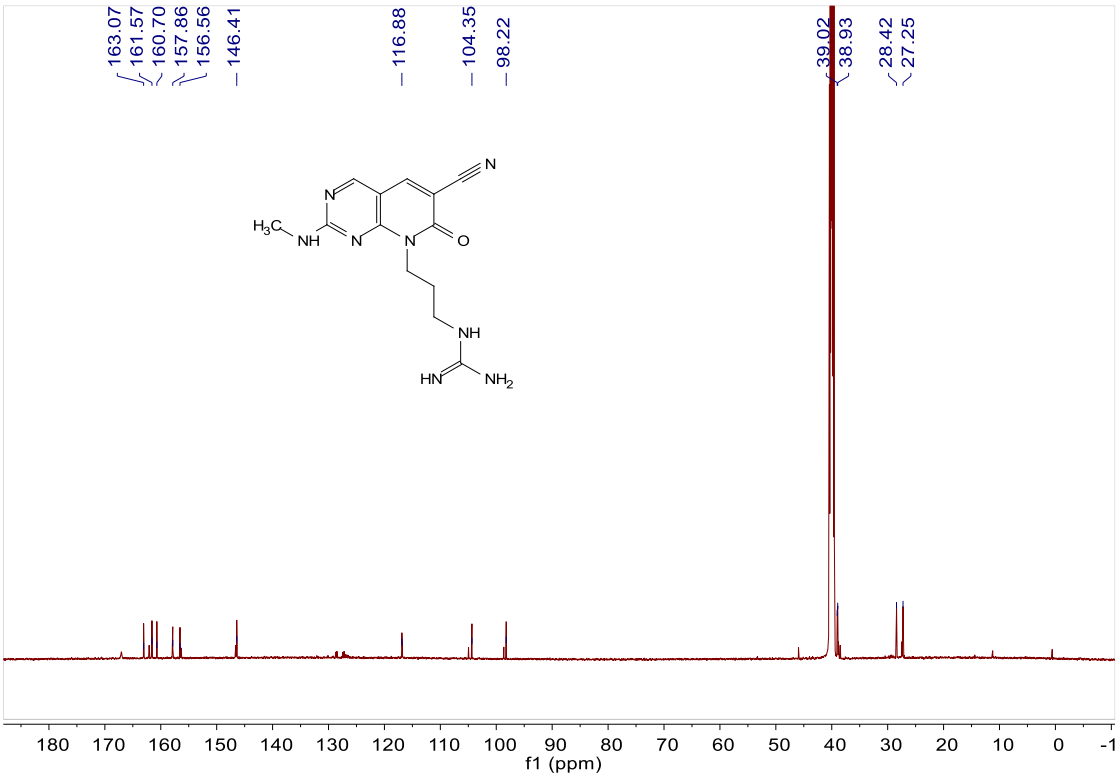

1-(2-(6-Cyano-2-((1-(methylsulfonyl)piperidin-4-yl)amino)-7-oxopyrido[2,3-*d*]pyrimidin-8(7H)-yl)ethyl)guanidine (**LL-DA-3**)

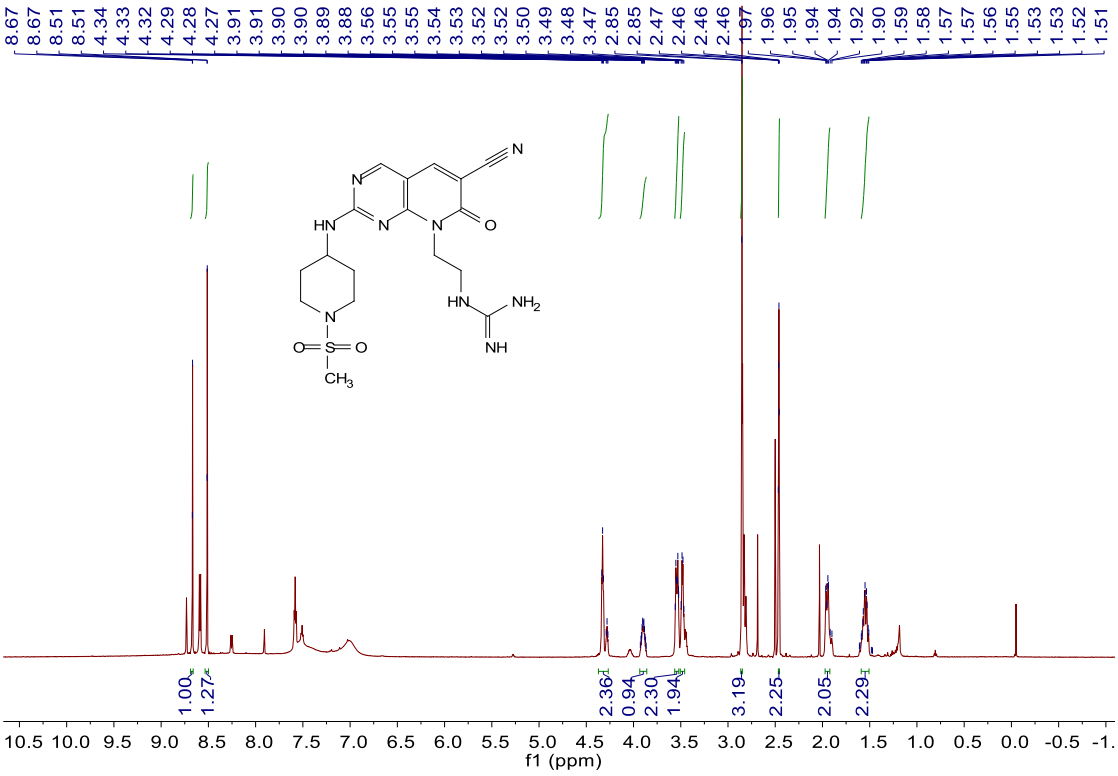

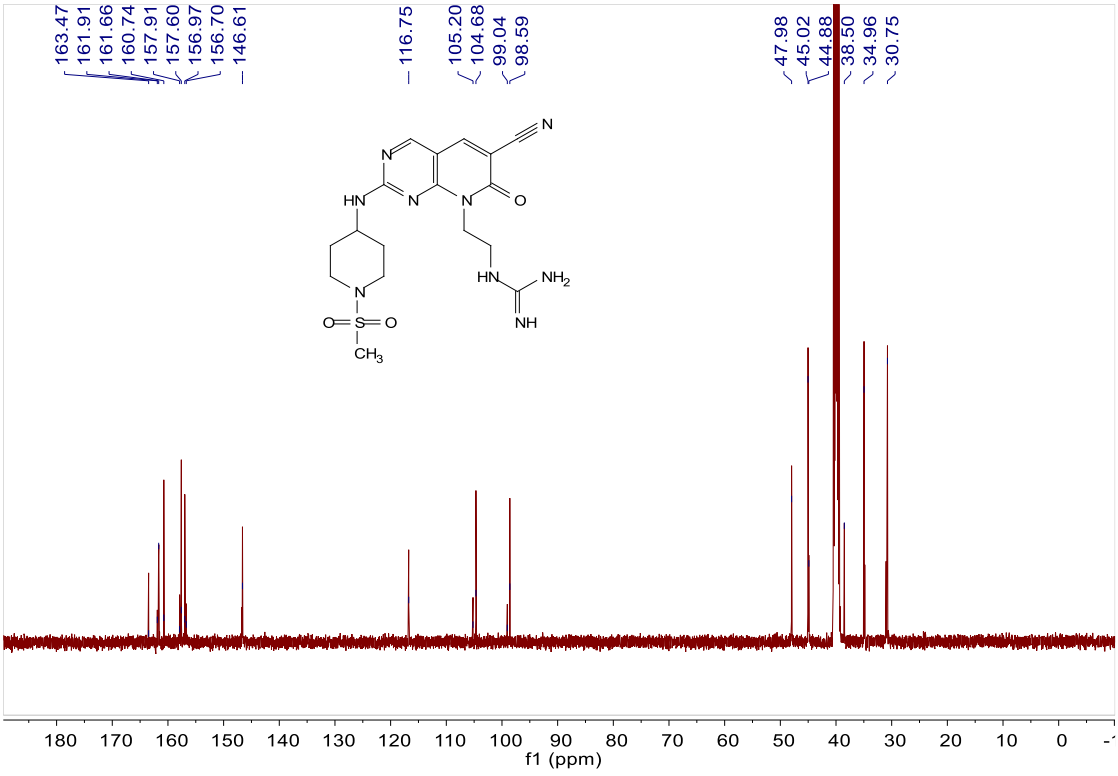

1-(3-(6-cyano-2-((1-(methylsulfonyl)piperidin-4-yl)amino)-7-oxopyrido[2,3-d]pyrimidin-8(7H)-yl)propyl)guanidine **(LL-DA-4)**

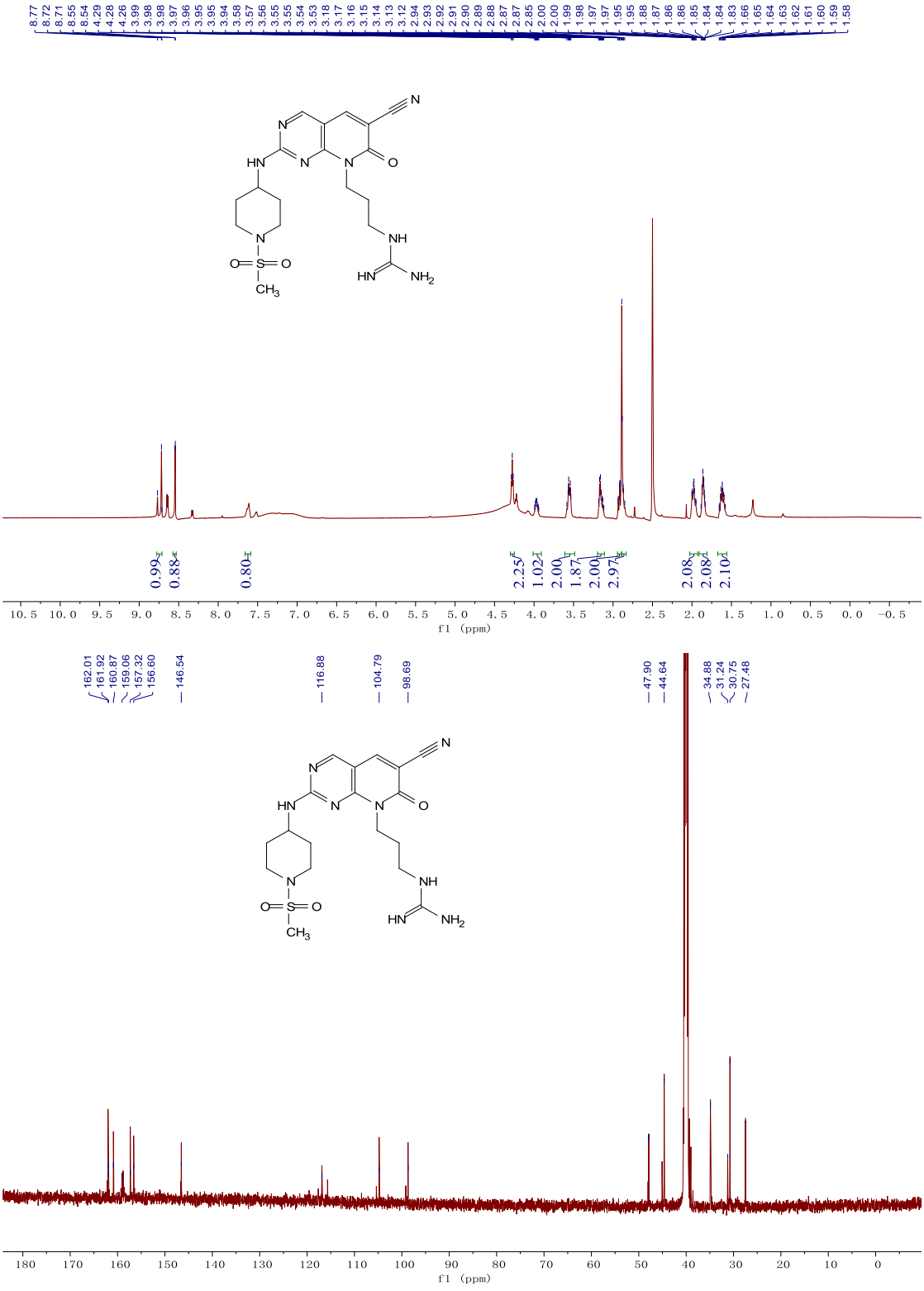

8-cyclopentyl-2-(methylamino)-7-oxo-7,8-dihydropyrido[2,3-*d*]pyrimidine-6-carbonitrile (**PC-4**)

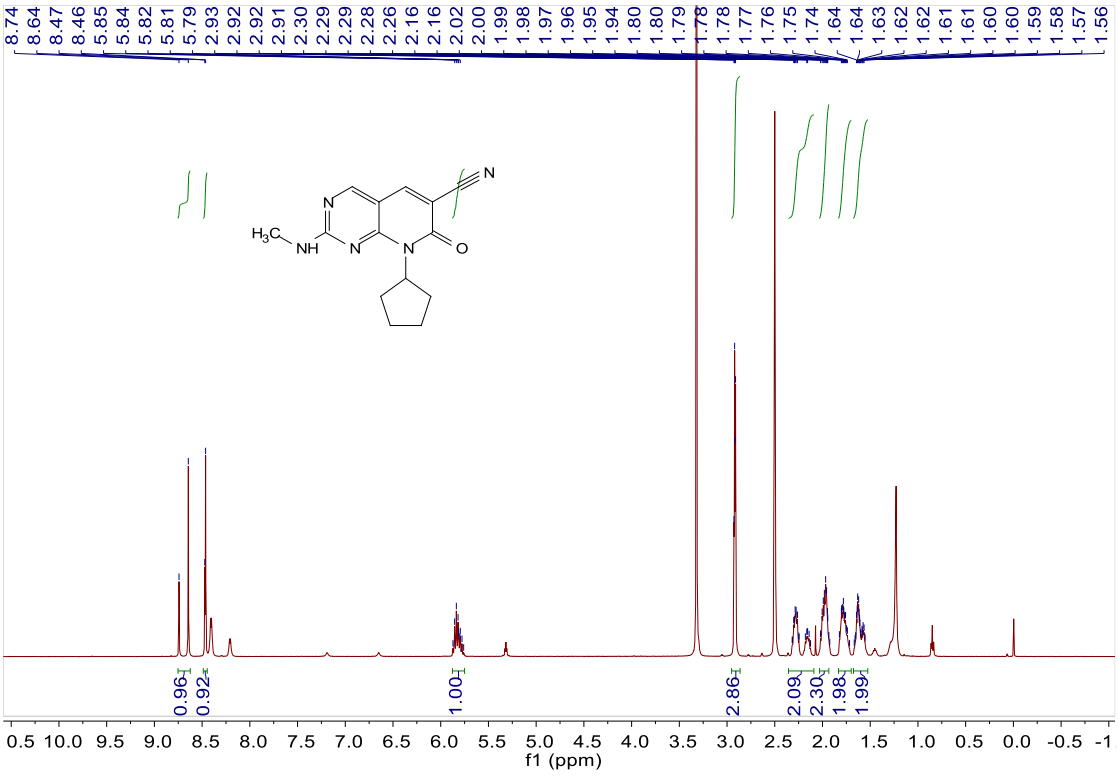

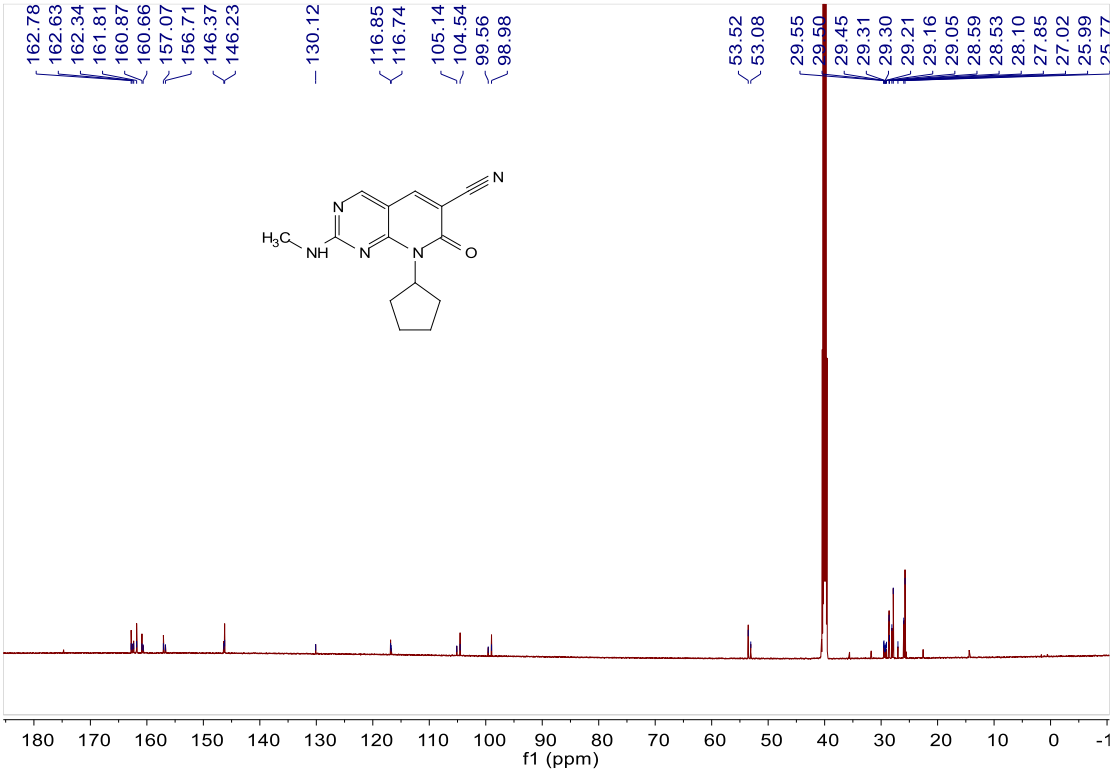

^{1}H NMR Spectrum of **a1**

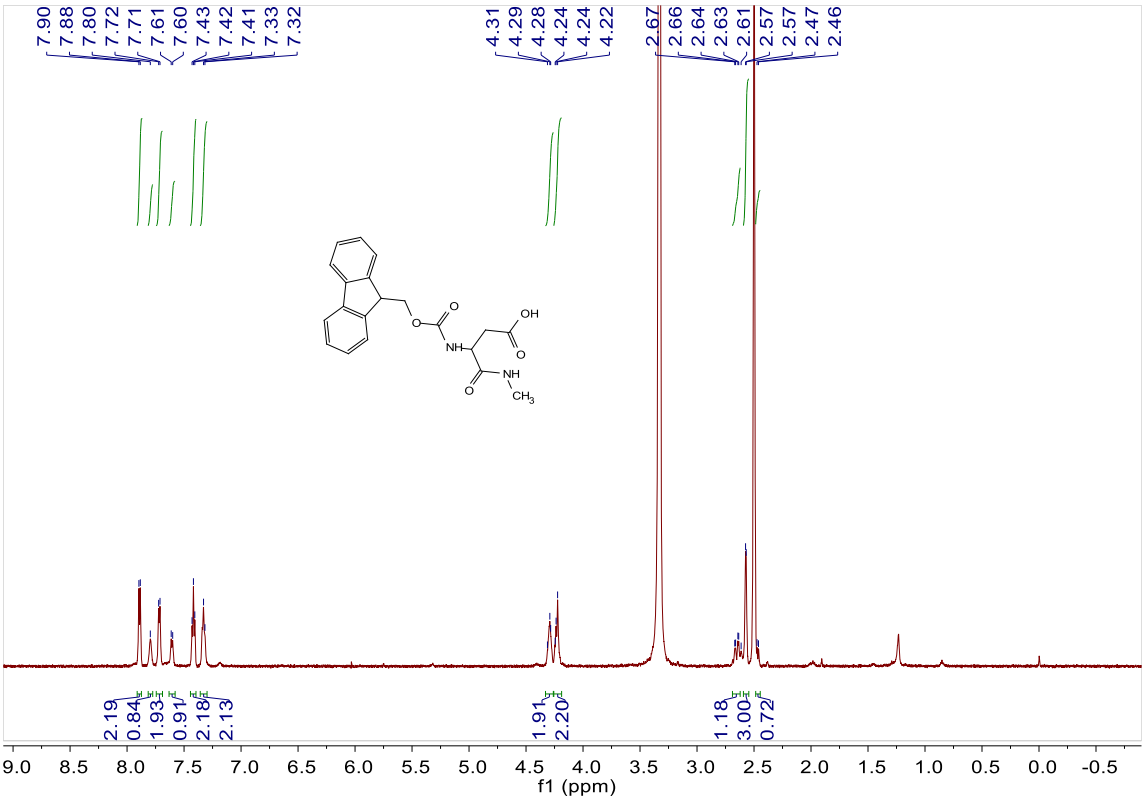

^{1}H NMR Spectrum of **b1**

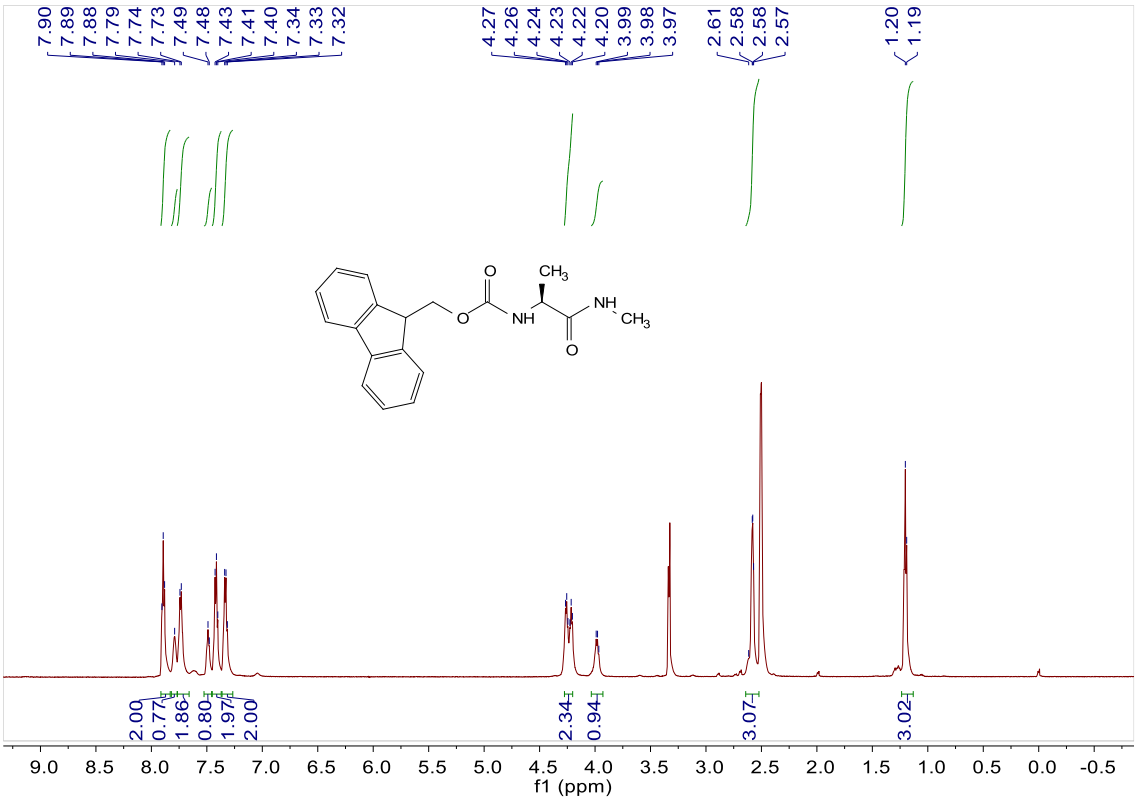

^{1}H NMR Spectrum of **a2**

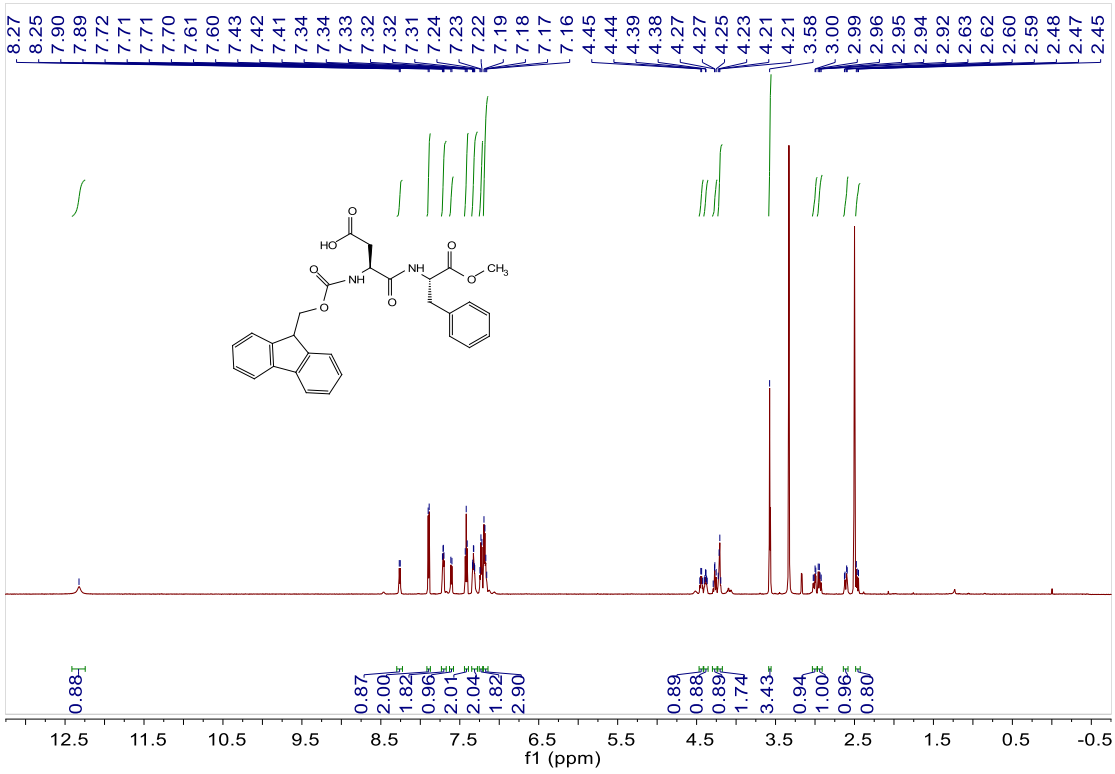

^{1}H NMR Spectrum of **b2**

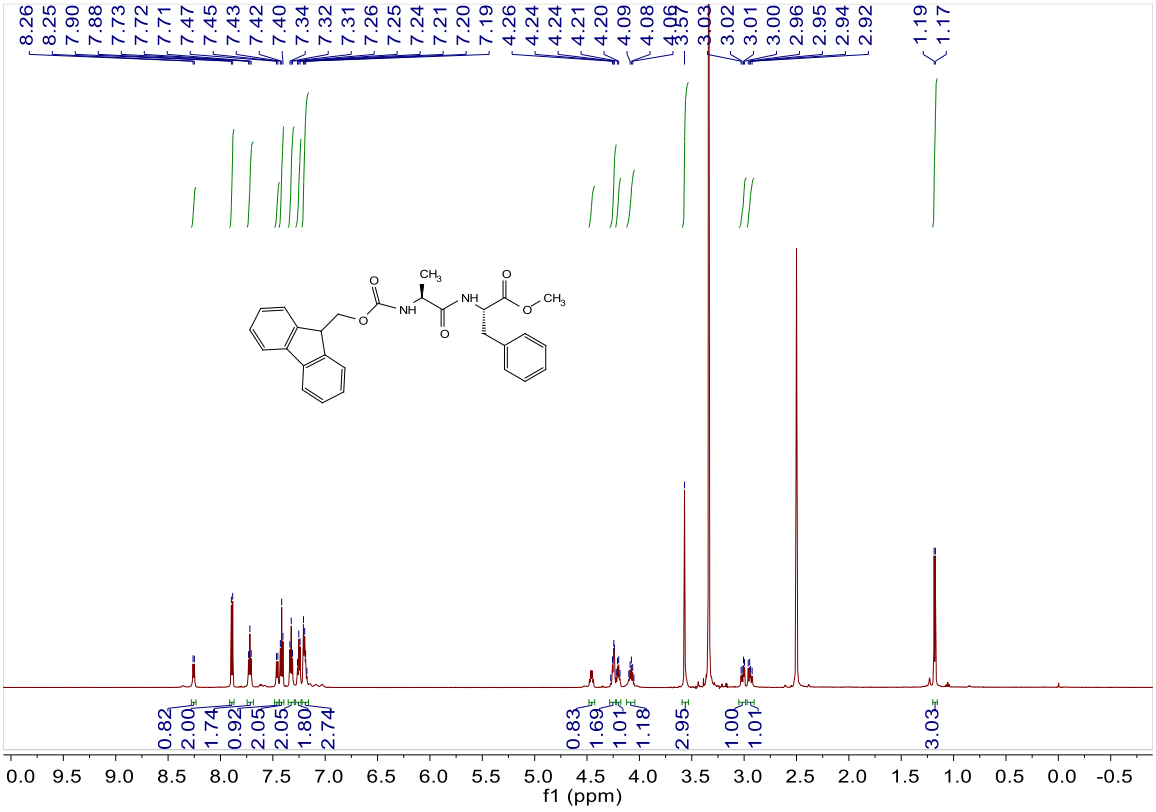

Typical procedure for photo-reaction

To a quartz tube were added substrate (**a1** or **a2**, 0.05 mmol), photocatalyst (PC, 0.01 mmol), 1-acetylguanidine (10.1 mg, 0.1mmol), DMF (2 mL) and 1×PBS buffer (pH = 7.2, 0.2 mL). Then, the tube was fitted with a rubber septum. After evacuation and N_2 backfilling for three times, the reaction mixture was irradiated by 400-405 nm LEDs (50 W) under N_2 atmosphere at room temperature for 10 hours. After reaction, the volume of reaction mixture was fixed to 25 mL by MeOH. The yield was determined *via* standard curve method by HPLC using 4-acetylpyridine (11 μL, 0.1 mmol) as internal standard.

Preparation of internal standard curve and determination of analyte concentrations

Different concentrations of **a1**, **b1**, **a2** and **b2** in MeOH (2 mM, 1 mM, 0.5 mM, 0.25 mM, 0.125 mM, 0.0625 mM) were prepared in 25 mL volumetric flasks with 4-acetylpyridine (11 μL, 0.1 mmol) as internal standard. 3 μL sample was injected into the UPLC with a Thermo Fisher Scientific Hypersil Gold column (5 μm, 2.1 × 100 mm) using a 0.1% aqueous formic acid/CH_3CN gradient (0.8 mL/min, an isocratic hold at 5% CH_3CN for 0.5 minutes, then 5–95% CH_3CN over 8 minutes followed by an isocratic hold at 95% CH_3CN for 1.5 minutes, 95–5% CH_3CN over 1 minute followed by an isocratic hold at 5% CH_3CN for 1 minute) at 25 °C.

Retention times for relevant compounds: **a1** 6.03 minutes (detection wavelength 254 nm), **b1** 6.35 minutes (detection wavelength 254 nm), **a2** 7.42 minutes (detection wavelength 254 nm), **b2** 7.83 minutes (detection wavelength 254 nm), 4-acetylpyridine 1.42 minutes (detection wavelength 254 nm).

Analyte concentrations were calculated against 4-acetylpyridine as internal standard, and all analytes were calibrated separately using a series of calibration solutions of different concentrations with the highest concentration of the series being 2 mM.

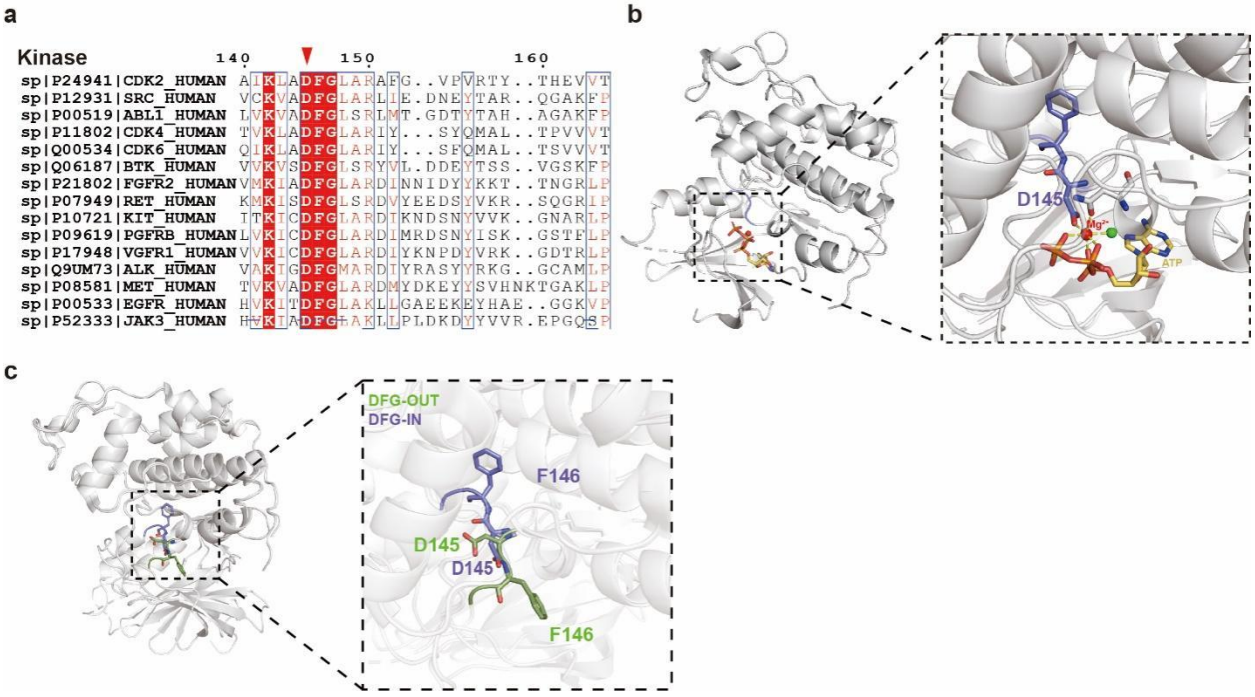

Supplementary Fig. 1| Background and motivation for small-molecule protein editing.
(**a**) Sequence alignment of the DFG motif in several typical human kinases. (**b**) The aspartate in the DFG motif is responsible for chelating the Mg^{2+} that orient the ATP for phospho-transfer. (**c**) The "DFG-in" and "DFG-out" conformations of kinase. The structural representation is based on coordinates from PDB entries 1hck and 5a14.[11, 12]

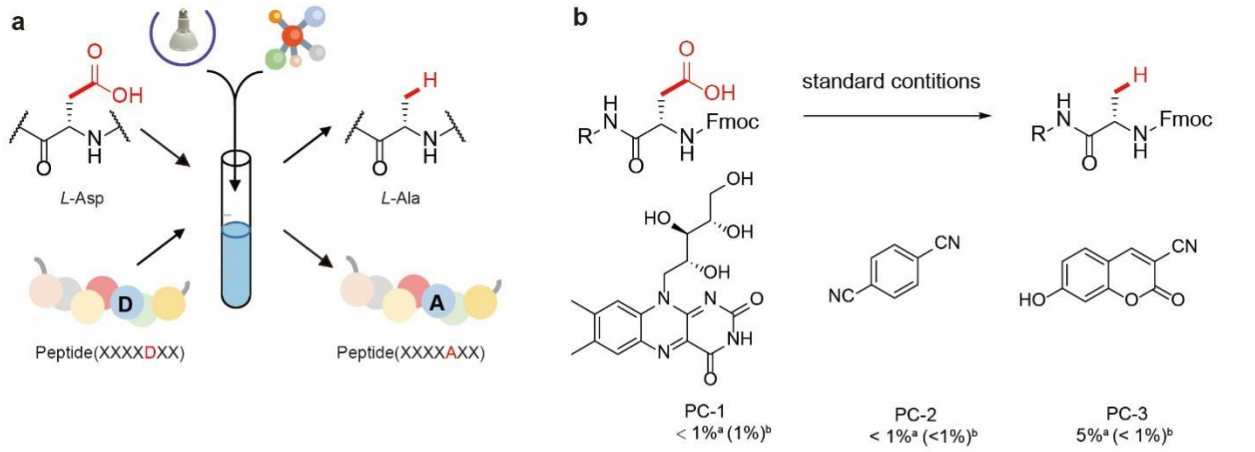

Supplementary Fig. 2| Development and application of LIDAPE for Protein Editing.
(**a**) Hydrodecarboxylation of the side chain of D at the amino acid and dipeptide levels. (**b**) Screening and optimization of LIDAPE for efficient decarboxylation[13]. Standard conditions: substrate (1 eq.), PC (20 mol%), 1-acetylguanidine (2 eq.), 400-405 nm (50 w), N_2 atmosphere, DMF:PBS = 10:1 (25 mM). a: R = Me, b: (S)-3-acetamido-4-(((S)-1-(methylamino)-1-oxo-3-phenylpropan-2-yl)amino)-4-oxobutanoic acid as substrate, c: PC (1 eq.) instead of (20 mol%), 1-acetylguanidine (1 eq.) instead of (2 eq.), DMF:PBS = 10:1 (5 mM) instead of (25 mM).

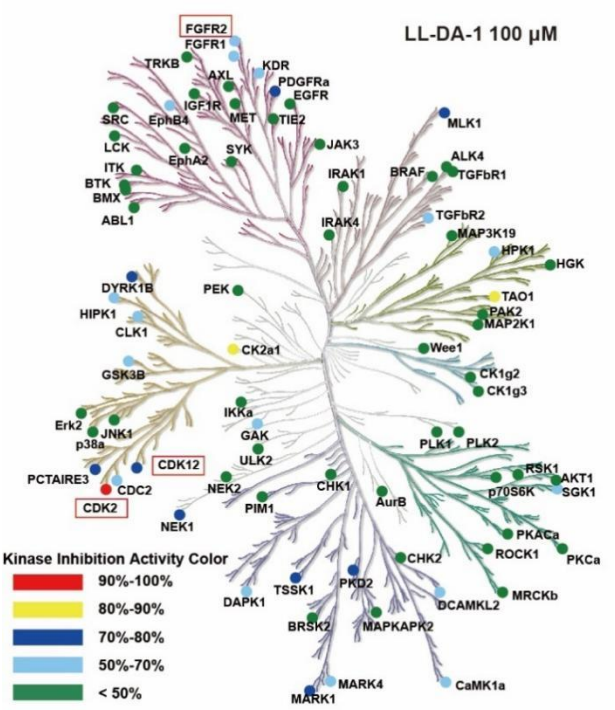

Supplementary Fig. 3| Inhibition profile of LL-DA-1.
Each kinase represented in the assay panel is marked with a circle. Different inhibitory activities are indicated by different colors. Examples of kinome tree annotation are created by KinMap.

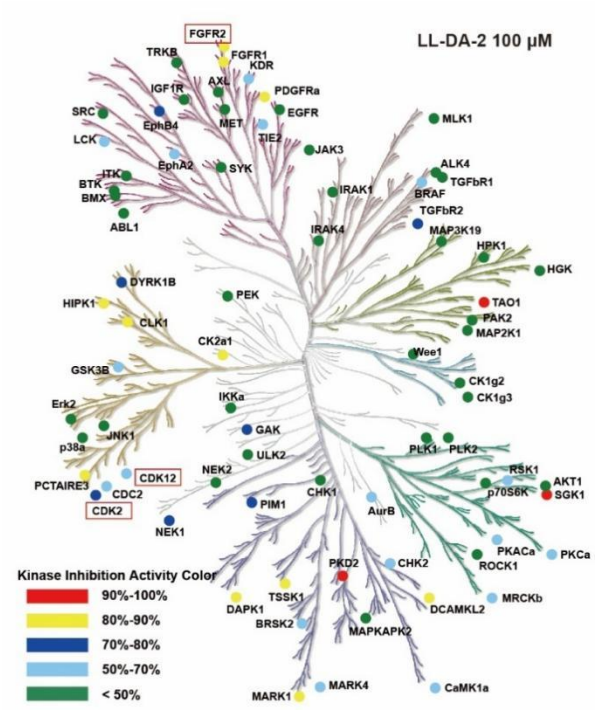

Supplementary Fig. 4| Inhibition profile of LL-DA-2.
Each kinase represented in the assay panel is marked with a circle. Different inhibitory activities are indicated by different colors. Examples of kinome tree annotation are created by KinMap.

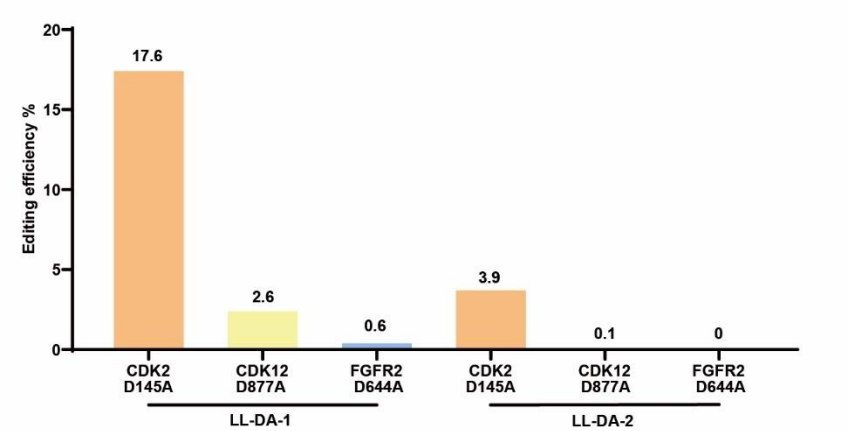

Supplementary Fig. 5| Editing efficiency of LL-DA-1 and LL-DA-2 on different kinases. **LL-DA-1/2** demonstrated editing activity at the aspartate residue of DFG motif across multiple kinases.

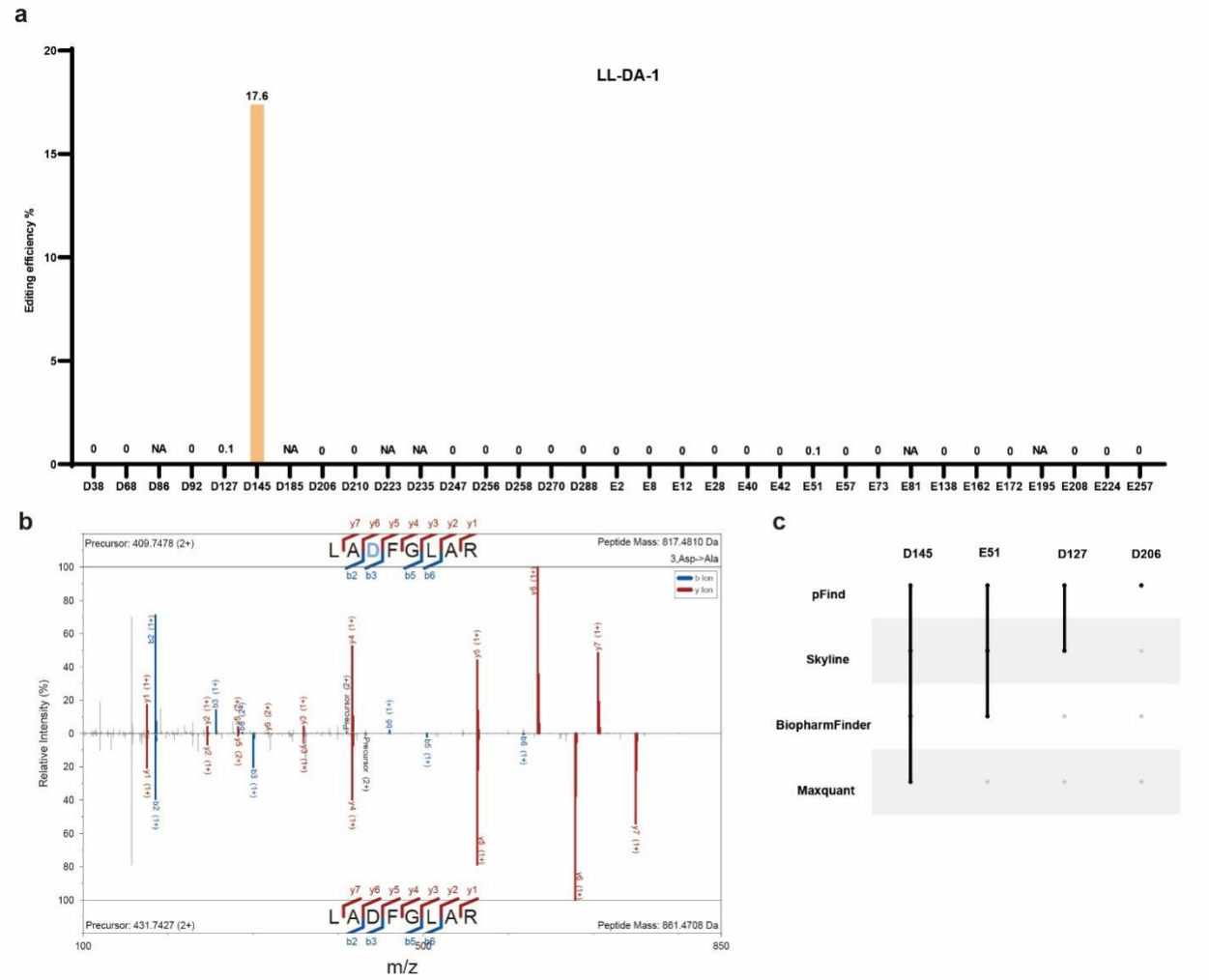

Supplementary Fig. 6| Site-selectivity profiling of LL-DA-1–mediated editing

(**a**)The editing efficiency of **LL-DA-1** across all D and E sites on CDK2. (**b**) Annotated MS/MS spectra of the unedited LADFGLAR (precursor m/z 431.7427, 2+) and edited LAD(Asp→Ala)FGLAR (precursor m/z 409.7478, 2+) peptides. (**c**) comparison of four search engines (pFind, Skyline, BiopharmFinder, MaxQuant) for −43.9898 Da events in CDK2; only D145 is consistently accepted at ⩽1% FDR.

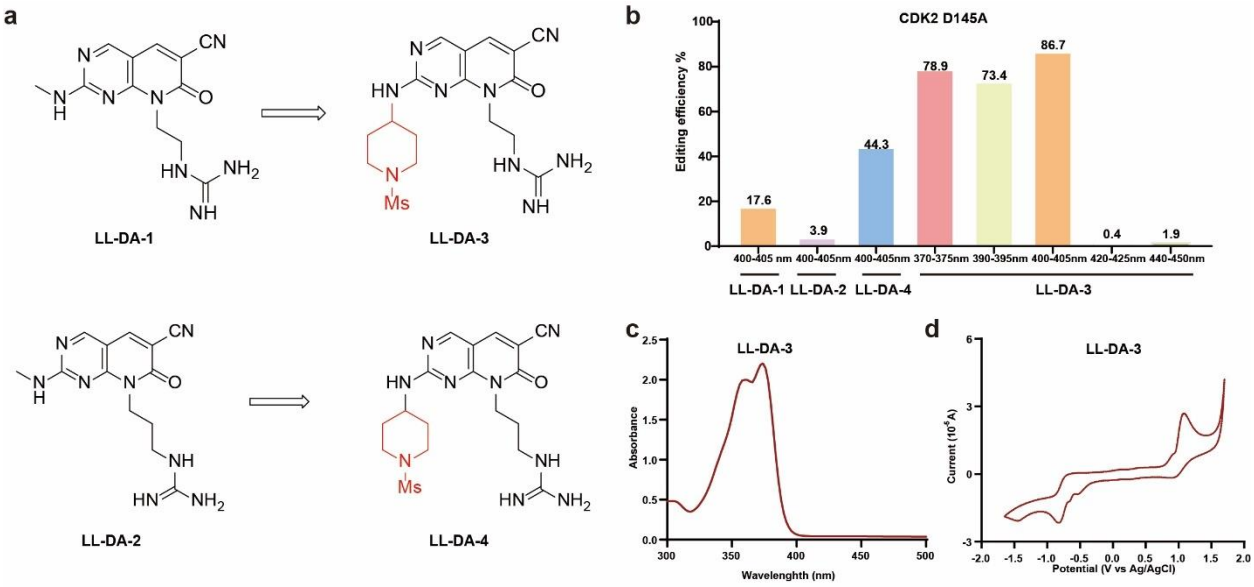

Supplementary Fig. 7| Optimization and application of LIDAPEs for CDK2 editing.
(**a**) Structural optimization of **LL-DA-3/4** for enhanced CDK2 binding and editing efficiency. (**b**) Effect of light wavelength on the editing efficiency of LL-DA-3. (**c**) Ultraviolet-visible spectra of **LL-DA-3**. (**d**) Cyclic voltammograms of **LL-DA-3**.

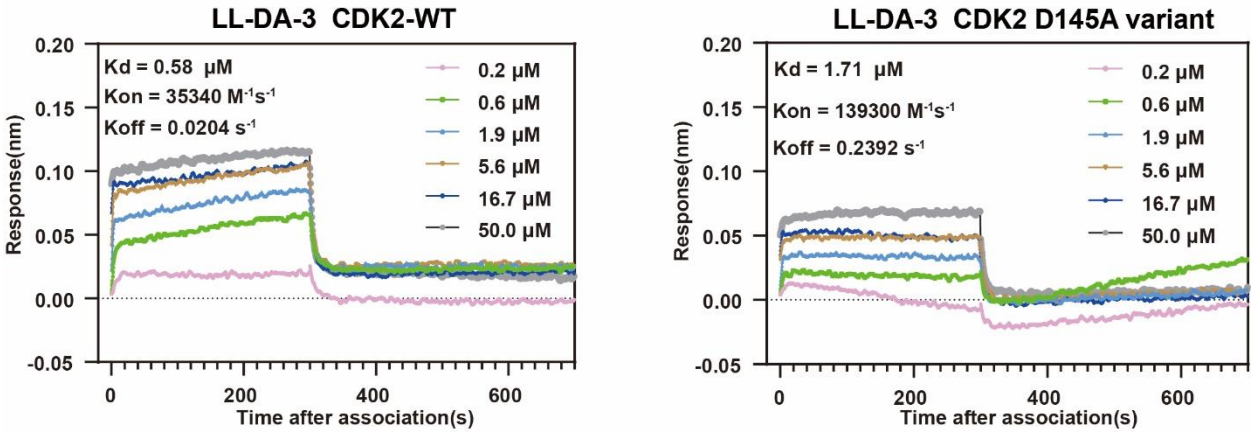

Supplementary Fig. 8| BLI experiments of wild-type CDK2 and D145A mutant CDK2 with LL-DA-3.
The sensorgrams revealed a concentration-dependent, rapid association and dissociation of the analyte with the immobilized ligand.

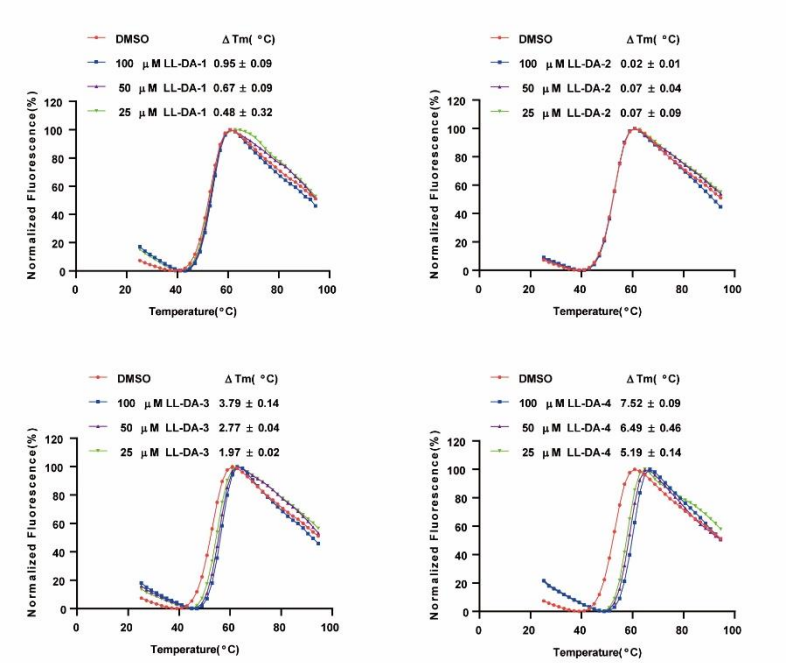

Supplementary Fig. 9| The effects of LL-DA-1~4 compounds on the thermal stability of CDK2

The effects of LL-DA compounds on the thermal stability of CDK2 were accessed by PTS experiments with three replicates. The figure shows a representative curve.

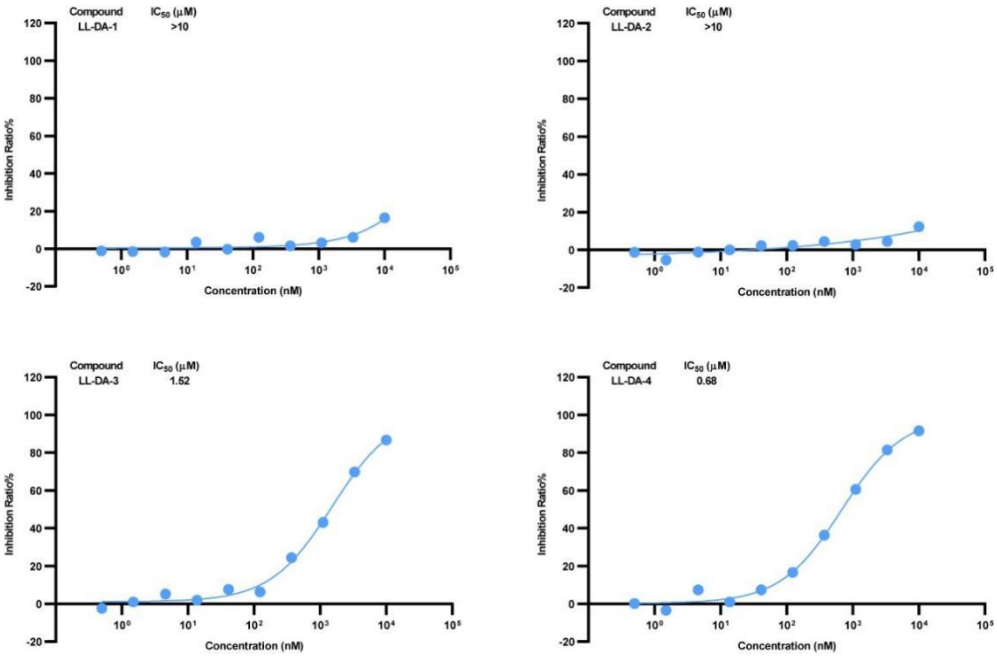

Supplementary Fig. 10| The inhibitory effects of LL-DA compounds on the CDK2 enzymatic activity.

The inhibitory effect of LL-DA compounds on the CDK2 enzymatic activity were accessed by Lance Ultra assay with CDK2-Cyclin E1 complex. The figure shows a representative curve.

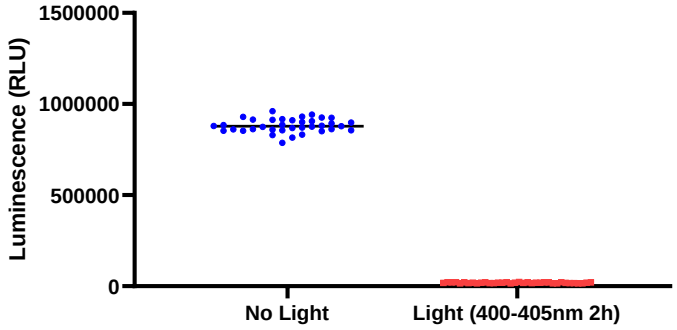

Supplementary Fig. 11| Cytotoxicity of light exposure on HEK-293T cells.
Cells were irradiated at 400-405 nm for 2 h without compound, and viability was directly assessed by CellTiter-Glo (CTG) luminescence.

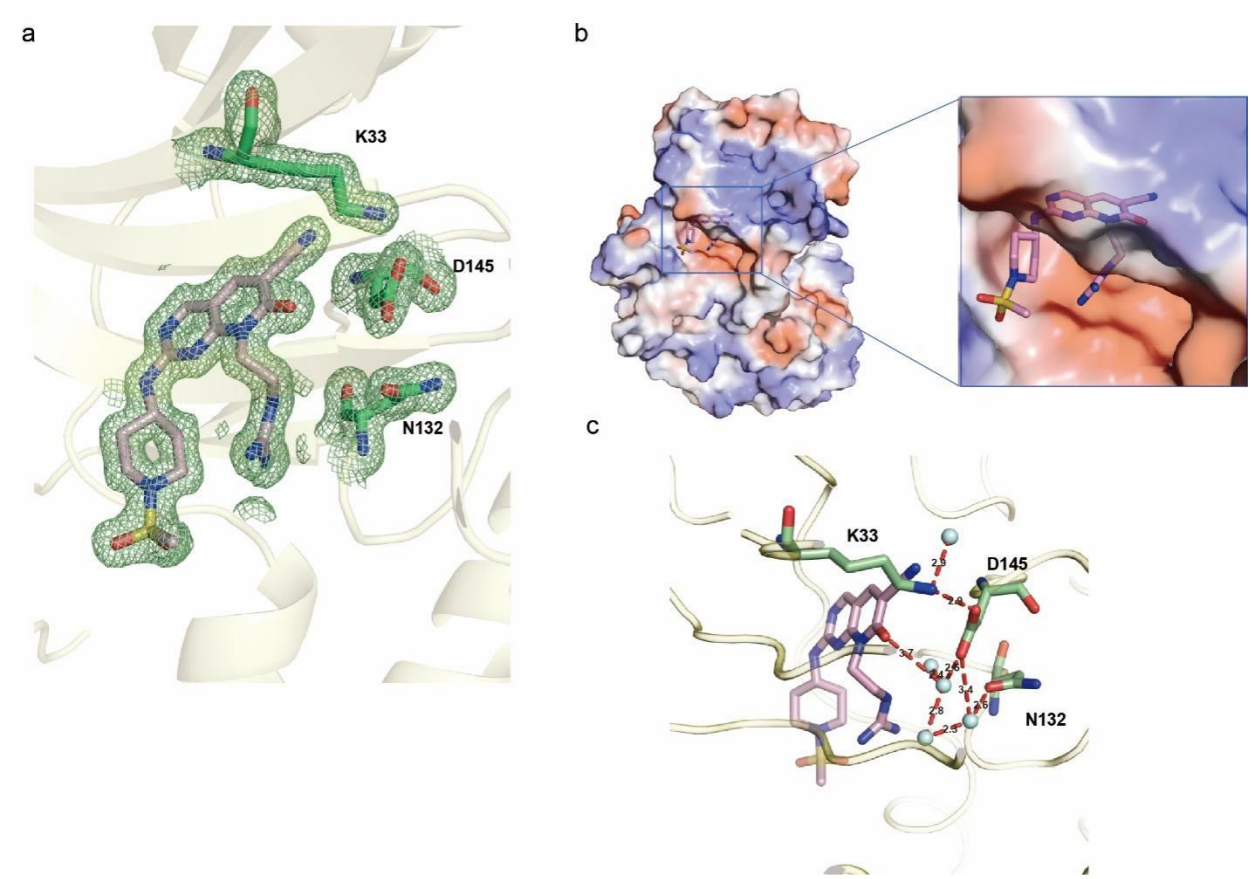

Supplementary Fig. 12| Crystal structure of CDK2 binding with LL-DA-3.
(**a**) The 2Fo-Fc density map for **LL-DA-3** and key amino acids, the contour level was set to 1.0 sigma. (**b**) Electrostatic surface of CDK2 binding with **LL-DA-3**. (**c**) The interaction network formed by **LL-DA-3**, conserved water molecules (pale cyan), and key amino acids. All distances are given in Ångstroms.

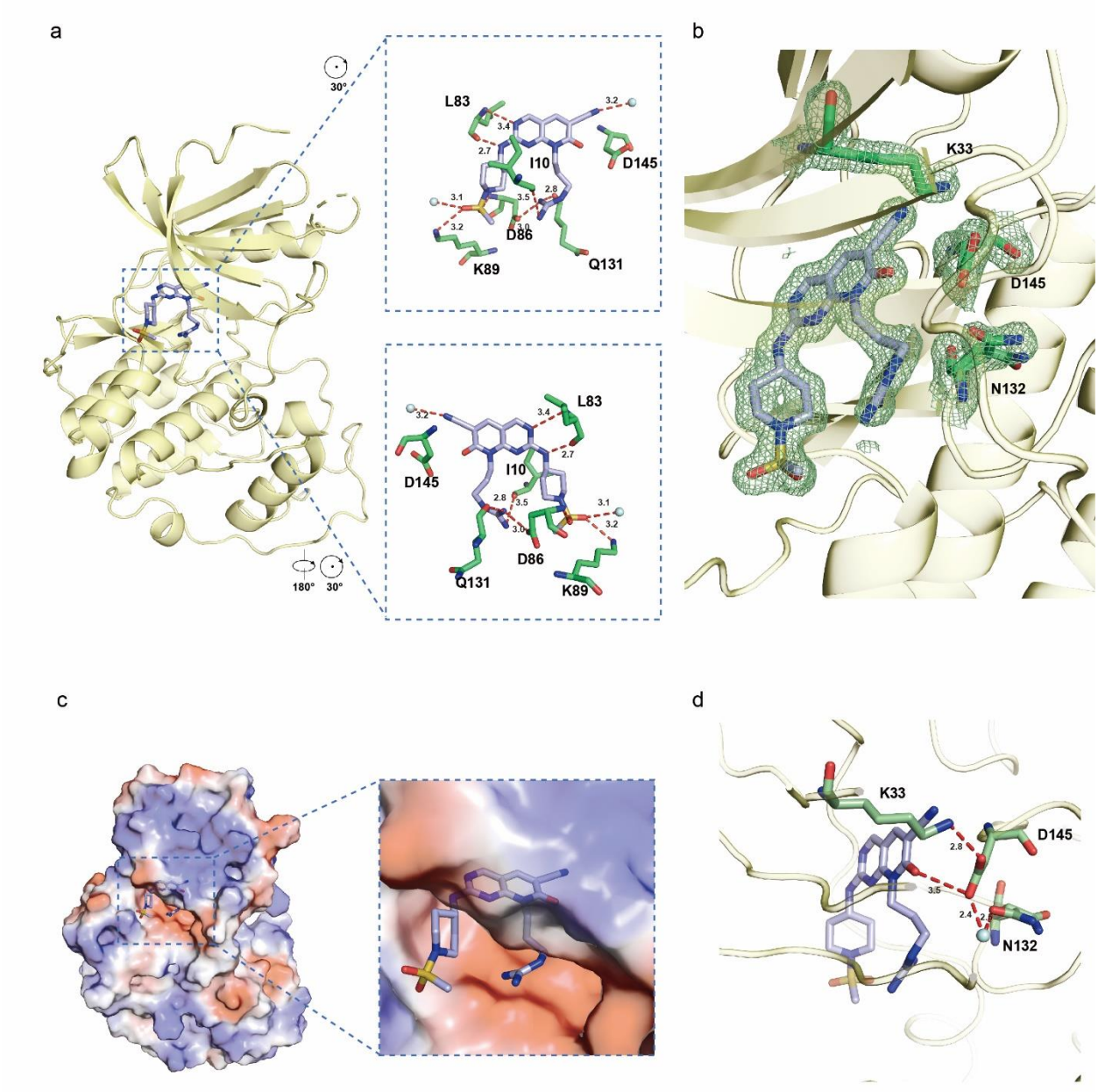

Supplementary Fig. 13| Crystal structure of CDK2 binding with LL-DA-4.
(**a**) Overall view of the crystal structure of CDK2 binding with **LL-DA-4**. **LL-DA-4** is shown in sticks mode with carbon atoms in slate. Detailed binding interactions of **LL-DA-4** and CDK2 are shown in the magnified view. Hydrogen bonds are shown in dashed red line. (**b**) The 2Fo-Fc density map for **LL-DA-4** and key amino acids, the contour level was set to 1.0 sigma. (**c**) Electrostatic surface of CDK2 binding with **LL-DA-4.** (**d**) The interaction network formed by **LL-DA-4**, conserved water molecules, and key amino acids. Conserved water molecules are shown in pale cyan. All distances are given in Ångstroms.

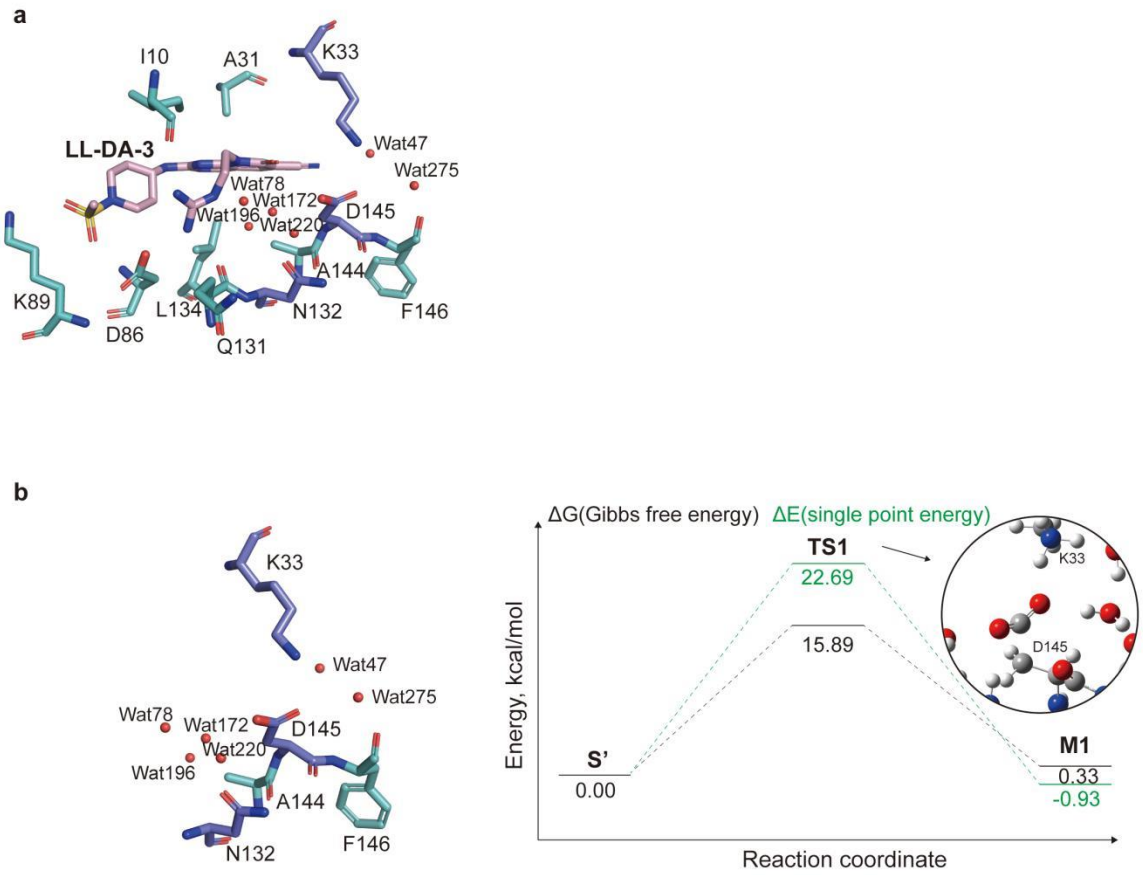

Supplementary Fig. 14| Cluster models in quantum chemical calculations and energy distribution of decarboxylation process.

(**a**) Model of the CDK2 active site. LL-DA-3, key residues and other residues are represented by white, purple and dark green sticks, respectively, and water molecules are represented by red spheres. (**b**) Left: Truncated model of the CDK2 active site in the radical state. Key residues are represented by purple sticks, other residues are represented by dark green sticks, and water molecules are represented by red spheres. Right: Energy distribution and optimized structure of transition states in the reaction obtained using UB3LYP-D3/6-311G** calculations. The black and green lines indicate the Gibbs energy and single-point energy, respectively.

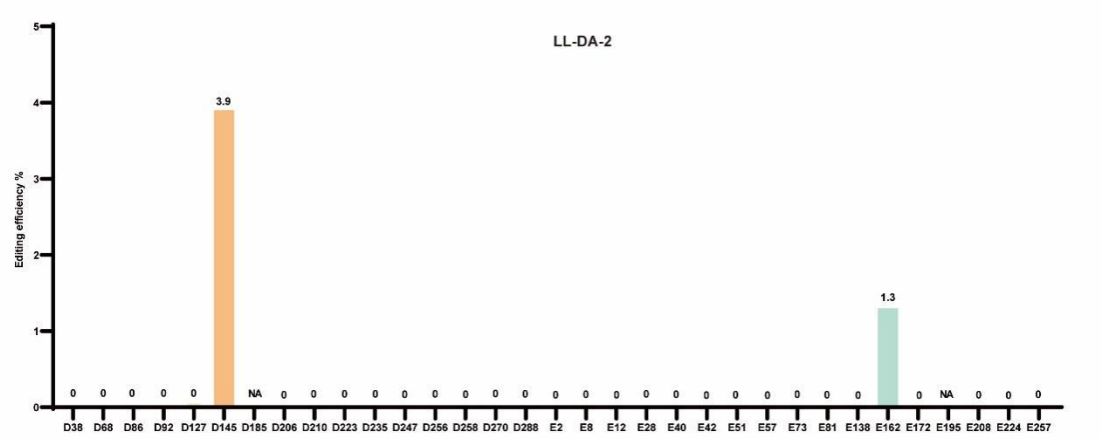

Supplementary Fig. 15| The editing efficiency of LL-DA-2 across all D and E sites on CDK2
The editing efficiency of **LL-DA-2** was quantified by LC-MS/MS across all detectable aspartate (D) and glutamate (E) residues in full-length CDK2.

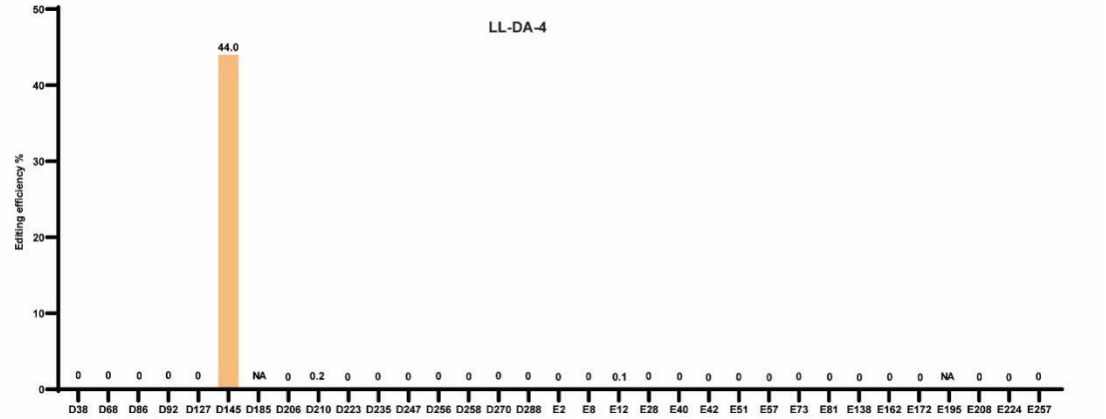

Supplementary Fig. 16| The editing efficiency of LL-DA-4 across all D and E sites on CDK2
The editing efficiency of **LL-DA-4** was quantified by LC-MS/MS across all detectable aspartate (D) and glutamate (E) residues in full-length CDK2.

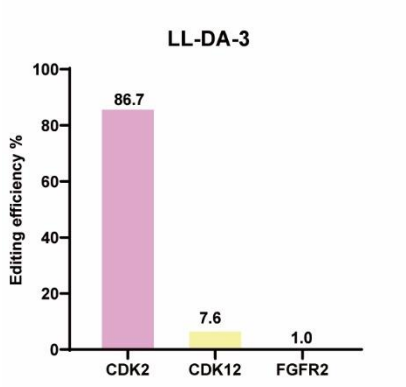

Supplementary Fig. 17| Editing efficiency of LL-DA-3 on different kinases (CDK2, CDK12, and FGFR2)

A editing efficiency of **LL-DA-3** was evaluated on the target aspartate residue within the DFG motif of CDK2 (D145), CDK12 (D877), and FGFR2 (D644). The results demonstrate the broad applicability of the editing platform across diverse kinases, while highlighting that the editing efficiency varies depending on the specific kinase target.

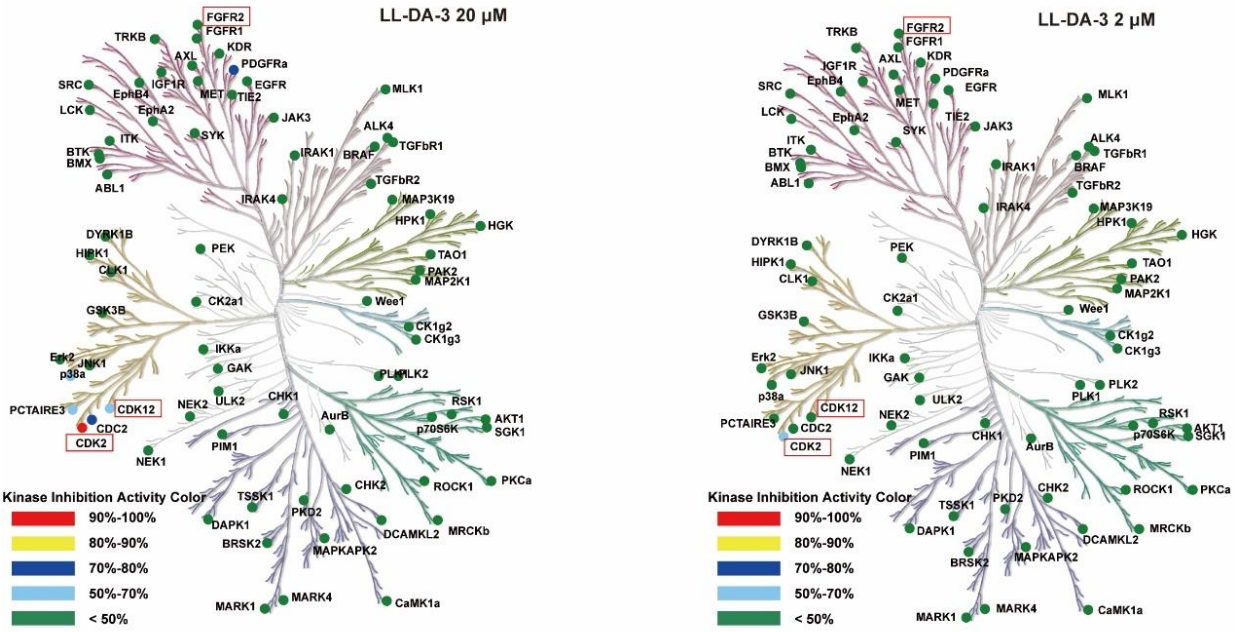

Supplementary Fig. 18| Inhibition profile of LL-DA-3

Each kinase represented in the assay panel is marked with a circle. Different inhibitory activities are indicated by different colors. Examples of kinome tree annotation are created by KinMap.

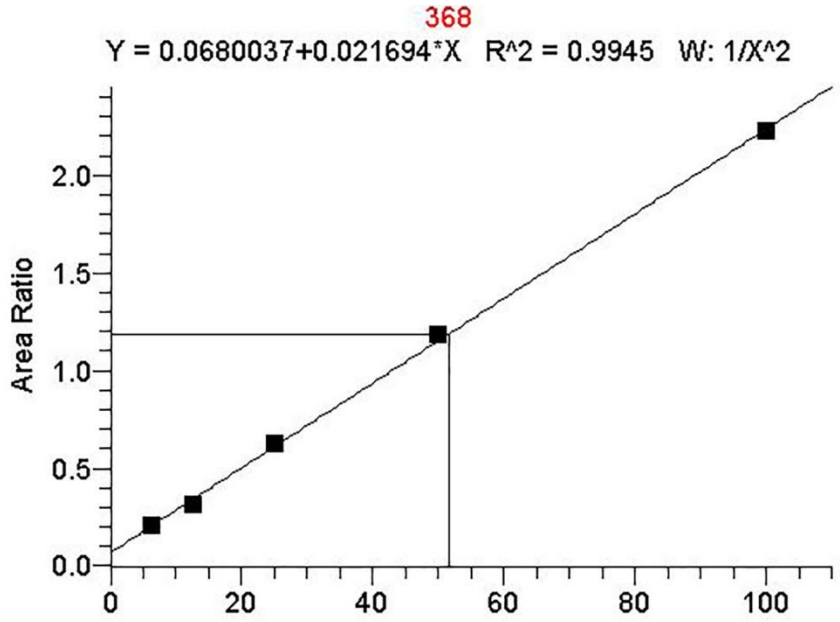

Supplementary Fig. 19| Standard curve of a1
Standard curve of a1 (retention time 6.03 minutes) was determined by UPLC using 4-acetylpyridine as internal standard.

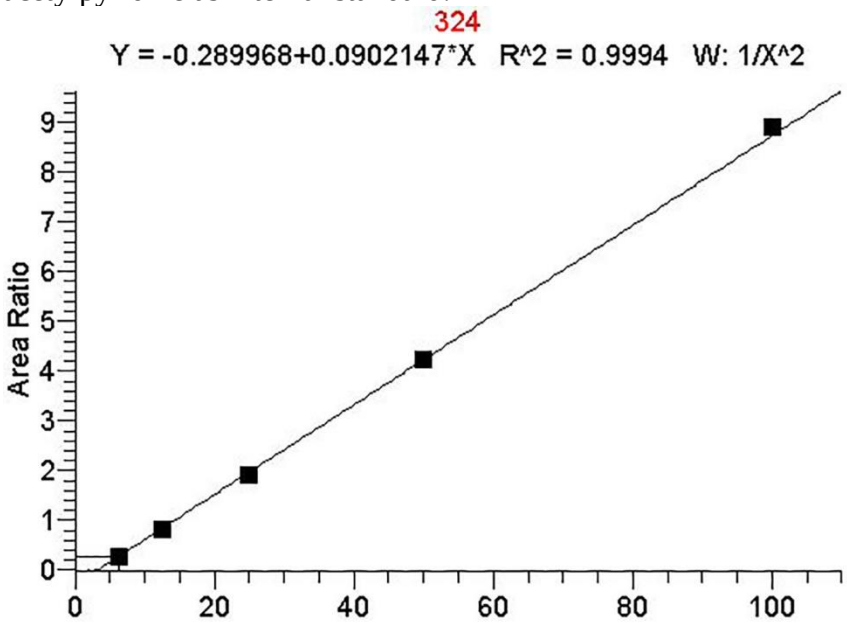

Supplementary Fig. 20| Standard curve of b1
Standard curve of b1 (retention time 6.35 minutes) was determined by UPLC using 4-acetylpyridine as internal standard.

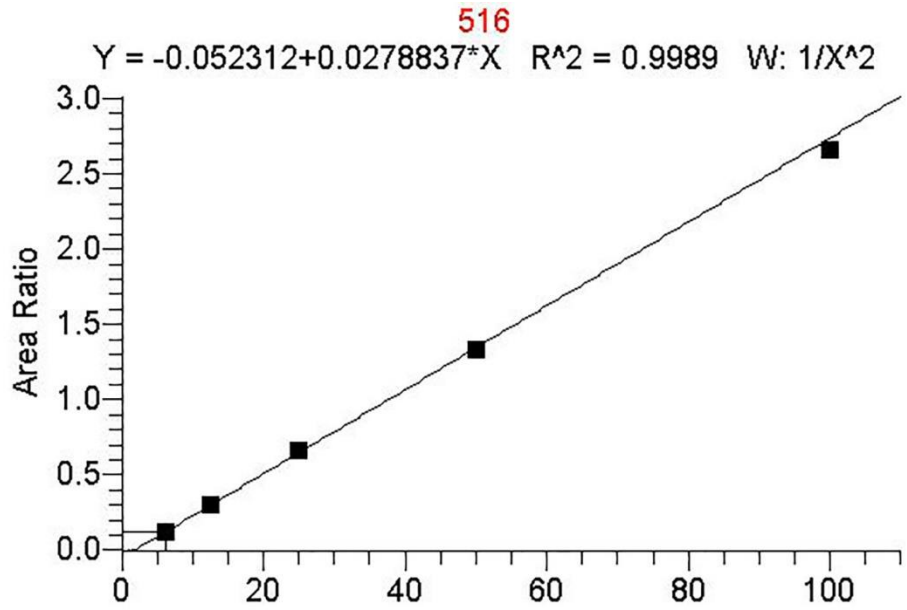

Supplementary Fig. 21| Standard curve of a2
Standard curve of a2 (retention time 7.42 minutes) was determined by UPLC using 4-acetylpyridine as internal standard.

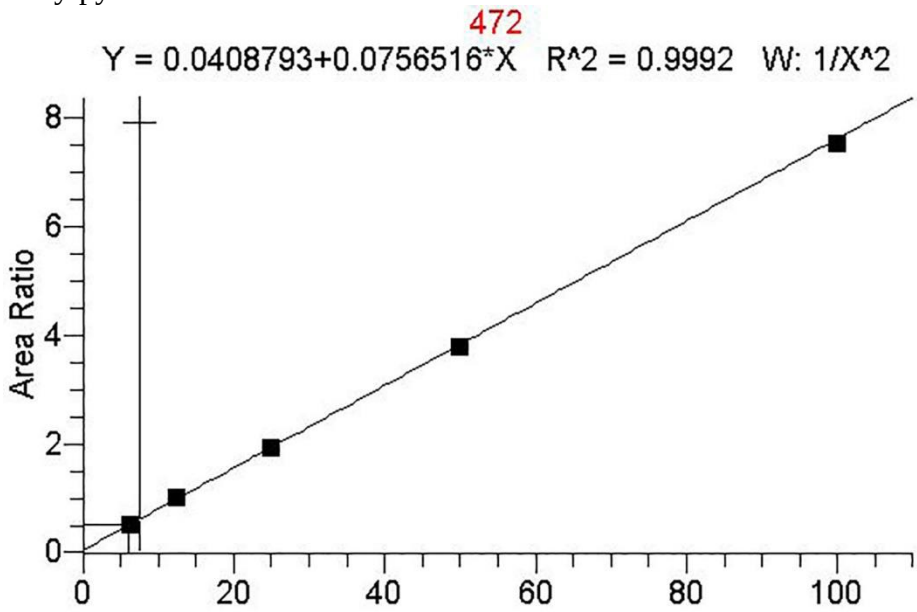

Supplementary Fig. 22| Standard curve of b2
Standard curve of b2 (retention time 7.83 minutes) was determined by UPLC using 4-acetylpyridine as internal standard

Supplementary Table 1| Optimization of wavelength[a]

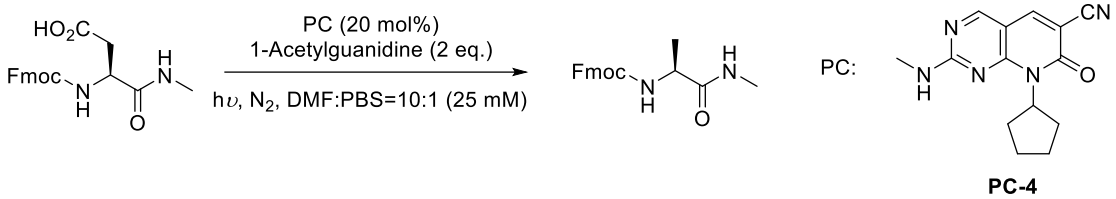

Entry	hν	Yield (HPLC)
1	385-390 nm	9%
2	400-405 nm	10%
3[b]	400-405 nm	trace
4	410-415 nm	8%
5	420-425 nm	<1%
6	430-435 nm	<1%

[a]Standard Conditions: substrate (0.05mmol, 1 eq.), PC (20 mol%), 1-acetylguanidine (2 eq.), irradiation (50 w), N_2 atmosphere, DMF:PBS = 10:1 (25 mM). [b]without 1-acetylguanidine as base.

Supplementary Table 2| Optimization of reaction time

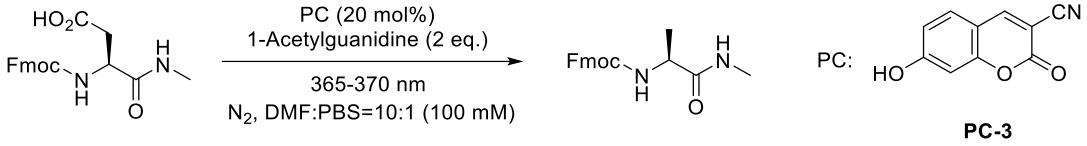

Entry	Reaction time (h)	Yield (HPLC)
1	1	trace
2	2	trace
3	4	trace
4	6	4 %
5	8	6 %
6	**12**	**8 %**
7	17	8 %

Conditions: substrate (0.05mmol, 1 eq.), PC (20 mol%), 1-acetylguanidine (2 eq.), 365-370 nm (50 w), N_2 atmosphere, DMF:PBS = 10:1 (100 mM).

Supplementary Table 3| The reduction potential of excited state

PC	Fluorescence emission peak (nm)	Excitation energy (eV)	Half-peak potential of reduction $E_{1/2}^{red}$ (V) vs. Ag/AgCl	Reduction potential of excited state Photocatalyst $E^*_{1/2}{}^{red}$ (V) vs. Ag/AgCl
PC-3	460	2.70	-0.821 V	1.879
PC-4	408	3.04	-0.775 V	2.265
LL-DA-1	409	3.03	-0.787 V	2.243
LL-DA-2	408	3.04	-0.778 V	2.262
LL-DA-3	410	3.02	-0.728 V	2.292
LL-DA-4	410	3.02	-0.757 V	2.263

Supplementary Table 4| The effect of thiol reducing agents on the editing ratio of LL-DA-3 on CDK2

Thiol reducing agents	/	1 mM DTT	1 mM TCEP
Editing Ratio (%) [a]	86.7	82.8	83.1

a. The editing reaction was performed under irradiation at 400–405 nm for 12 h at 4°C.

Supplementary Table 5| The effect of GSH on the editing ratio of LL-DA-3 on CDK2

Intracellular reductant	/	1 mg / L GSH	1 g / L GSH
Editing Ratio (%)	86.7	82.8	82.8

The editing reaction was performed under irradiation at 400–405 nm for 12 h at 4°C.

Supplementary Table 6| X-ray Diffraction Data Collection and Refinement Statistics

	CDK2+LL-DA-3 （PDB: 9UAU）	CDK2+LL-DA-4 （PDB: 9UAW）
Resolution range	42.9 - 1.47 (1.523 - 1.47)	43.1 - 1.72 (1.782 - 1.72)
Space group	P 21 21 21	P 21 21 21
Unit cell	53.62 71.4 71.84 90 90 90	53.8 72 72.21 90 90 90
Total reflections	85713 (4707)	60932 (5958)
Unique reflections	42981 (2398)	30466 (2979)
Multiplicity	2.0 (2.0)	2.0 (2.0)
Completeness (%)	90.25 (51.21)	99.91 (99.90)
Mean I/sigma(I)	27.14 (1.99)	13.62 (1.88)
Wilson B-factor	18.52	20.46
R-merge	0.01255 (0.3662)	0.0302 (0.4045)
R-meas	0.01774 (0.5179)	0.04271 (0.5721)
R-pim	0.01255 (0.3662)	0.0302 (0.4045)
CC1/2	1 (0.739)	0.999 (0.821)
CC*	1 (0.922)	1 (0.95)
Reflections used in refinement	42978 (2398)	30449 (2977)
Reflections used for R-free	2008 (111)	1991 (196)
R-work	0.1863 (0.2694)	0.1968 (0.2847)
R-free	0.2188 (0.3479)	0.2483 (0.2689)
CC(work)	0.960 (0.852)	0.959 (0.904)
CC(free)	0.949 (0.724)	0.924 (0.873)
Number of non-hydrogen atoms	2739	2630
macromolecules	2433	2399
ligands	53	56
solvent	276	200
Protein residues	303	298
RMS(bonds)	0.037	0.064
RMS(angles)	1.56	0.91
Ramachandran favored (%)	97.01	96.94
Ramachandran allowed (%)	2.66	3.06
Ramachandran outliers (%)	0.33	0.00
Rotamer outliers (%)	0.00	0.00
Clashscore	5.66	7.37
Average B-factor	25.80	29.67
macromolecules	25.23	29.45
ligands	18.07	22.97
solvent	31.68	33.34

Supplementary Table 7|. Editing ratio of LL-DA-1 and LL-DA-2 on multiple kinase targets (CDK2, CDK12, FGFR2) at 4 °C and 25 °C

Compound	CDK2 D145A Editing Ratio (%)		CDK12 D877A Editing Ratio (%)		FGFR2 D644A Editing Ratio (%)	
	4 ℃	25 ℃	4 ℃	25 ℃	4 ℃	25 ℃
LL-DA-1	17.6	12.0	2.6	1.0	0.6	0.3
LL-DA-2	3.9	3.9	0.1	0.2	0	0

The editing reaction was performed under irradiation at 400–405 nm for 12 h at 4°C.

Reference

1 Xiao QJ. *et al*. *J Appl Crystallogr* 2024; **57**:630-637.
2 Wisniewski JR. *et al*. *Nat Methods* 2009; **6**:359-362.
3 Fang Z. *et al*. *Genomics Proteomics Bioinformatics* 2024; **22**.
4 Himo F. *J Am Chem Soc* 2017; **139**:6780-6786.
5 Cassimjee KE. et al. *Org Biomol Chem* 2015; **13**:8453-8464.
6 Grimme S. et al. *J Chem Phys* 2010; **132**:154104.
7 Grimme S. et al. *J Comput Chem* 2011; **32**:1456-1465.
8 Frisch MJ. et al. Gaussian 16 Rev. A.03. Wallingford, CT 2016.
9 Lu T. et al. *Comput Theor Chem* 2021; **1200**:113249.
10 Ho J. et al. *J Phys Chem A* 2010; **114**:13442-13444.
11 Alexander LT. et al. *ACS Chem Biol* 2015; **10**:2116-2125.
12 Schulze-Gahmen U. et al. *J Med Chem* 1996; **39**:4540-4546.
13 Shinkawa Y. et al. *J Org Chem* 2022; **87**:11816-11825.